United States
Environmental Protection
Agency

Environmental Research
Laboratory
Narragansett RI 02882

EPA-600/3-80-011
January 1980

Research and Development

EPA

Adsorption of Trace Metals by Hydrous Ferric Oxide in Seawater

EPA-600/3-80-011
January 1980

ADSORPTION OF TRACE METALS BY HYDROUS FERRIC OXIDE IN SEAWATER

K. C. Swallow and Francois Morel
Ralph M. Parsons Laboratory
For Water Resources and Hydrodynamics
Department of Civil Engineering
Massachusetts Institute of Technology
Cambridge, Massachusetts 02139

Grant R-803738

Project Officer

Earl W. Davey
Environmental Research Laboratory
Narragansett, Rhode Island 02882

ENVIRONMENTAL RESEARCH LABORATORY
OFFICE OF RESEARCH AND DEVELOPMENT
U.S. ENVIRONMENTAL PROTECTION AGENCY
NARRAGANSETT, RHODE ISLAND 02882

DISCLAIMER

This report has been reviewed by the Environmental Research Laboratory, Narragansett, U. S. Environmental Protection Agency, and approved for publication. Approval does not signify that the contents necessarily reflect the views and policies of the U. S. Environmental Protection Agency, nor does mention of trade names or commercial products constitute endorsement or recommendation for use.

FOREWORD

The Environmental Research Laboratory of the U.S. Environmental Protection Agency is located on the shore of Narragansett Bay, Rhode Island. In order to assure the protection of marine resources, the laboratory is charged with providing a scientifically sound basis for Agency decisions on the environmental safety of various uses of marine systems. To a great extent, this requires research on the tolerance of marine organisms and their life stages as well as of ecosystems to many forms of pollution stress. In addition, a knowledge of pollutant transport and fate is needed.

This report describes a three-year project aimed at improving modelling capabilities for the fate of metallic waste constituents in coastal waters. The particular focus of the report is the study of metal adsorption onto hydrous ferric oxide.

Donald K. Phelps
Acting Director, ERLN

PREFACE

Assessment of the environmental impact of activities which alter the chemical characteristics of a body of water is made especially difficult by the great number and complexity of the possible reactions through which a chemical can be mobilized or precipitated and can take biologically active--sometimes toxic--or inactive forms. One approach to such a problem is to build reasonable models of the systems under study by assembling all relevant thermodynamic, kinetic and analytical information. In this fashion at least "chemical boundary conditions" can be established that permit the isolation of the essential processes and point the way to relevant research on smaller and more manageable experimental systems.

This report describes a three year project aimed at improving our modelling capabilities for the fate of metallic waste constituents in coastal waters. The particular focus of the report is the study of metal adsorption onto hydrous ferric oxide. This process was singled out as the one whose ignorance was most responsible for the inadequacies of our present thermodynamic modelling of the metal chemistry in waste fields.

As part of the same project, new computer programs for chemical calculations have been developed. These (particularly the MINEQL series) have been widely distributed among universities, industry and government research centers and are used routinely for environmental studies. A particular focus of the modelling effort has focussed on the question of alternative models for adsorption of solutes at solid water interfaces.

The following reports and publications should be consulted for specifics regarding these various models:

MINEQL, A Computer Program for the Calculation of Chemical Equilibrium Composition of Aqueous Systems. J.C. Westall, J.L. Zachary, F.M.M. Morel. 1976. Water Quality Laboratory, Ralph M. Parsons Laboratory for Water Resources and Environmental Engineering, Department of Civil Engineering, Massachusetts Institute of Technology, Cambridge, MA 02138. Technical Note No. 18.

The Use and Abuse of MINEQL-II. J.L. Zachary. 1977. Ralph M. Parsons Laboratory for Water Resources and Environmental Engineering, Department of Civil Engineering, Massachusetts Institute of Technology, Cambridge, MA 02138.

Morel, F.M.M., J.G. Yeasted, J.C. Westall. "Adsorption Models: A Mathematical Analysis in the Framework of General Equilibrium Calculations", In: M.A. Anderson and A. Rubin [eds.], Adsorption of Inorganics at the Solid-Liquid Interface. Ann Arbor Science, Ann Arbor,

Michigan. 1979 (in press).

Chemical Equilibrium Including Adsorption on Charged Surfaces. J.C. Westall. 1979 (in press). Swiss Federal Institute of Technology, EAWAG, CH-8600, Duebendorf, Switzerland.

ABSTRACT

The adsorption of trace metals by amorphous hydrous ferric oxide in seawater is studied with reference to simple model systems designed to isolate the factors which may have an effect on the isotherms. Results show that the complex system behaves in a remarkably simple way and that the data obtained under various conditions of total metal concentration and total oxide concentration can be reduced to an apparent reaction constant, K, which is a function of pH only. The high capacity of the oxide for trace metals renders the concept of a surface reaction useless to explain the uptake of metals. A physical picture of the oxide as a swollen hydrous gel permeable to hydrated ions is presented.

This report was submitted in fulfillment of Grant Number R-803738 under the sponsorship of the Environmental Protection Agency. The work cited in this report was completed as of April 1978 and is included in the Ph.D thesis of Kathleen C. Swallow (Massachusetts Institute of Technology, 1978). This work has also been submitted (July 1979) for publication to the journal, Environmental Science and Technology in a paper entitled, "Sorption of Copper and Lead by Hydrous Ferric Oxide" by K.C. Swallow, D.N. Hume and F.M.M. Morel.

CONTENTS

FIGURES

TABLES

SECTION 1

BACKGROUND

INTRODUCTION

A comparison of the measured concentrations of trace metals in seawater with calculations of the solubilities of the least soluble compounds which can be formed from trace metals and the major components of seawater has led to the conclusion that seawater is undersaturated with respect to many trace elements (1,2,3). Various mechanisms for removal of trace metals to the sediments have been proposed as the controlling factor for their concentrations in seawater. Krauskopf (1) performed a series of simple experiments to test the efficiency of a number of processes for removing trace metals to a solid phase: precipitation as the least soluble species, precipitation by sulfides and adsorption by ferrous sulfide in reducing environments, and adsorption on hydrous ferric oxide, hydrous manganese oxide, apatite, clay and organic matter. He concluded that adsorption on one or more of these substrates could account for the low aqueous concentrations of eight of thirteen metals studied. In particular, hydrous ferric oxide removed 95% of the Zn, 98% of the Cu, 92% of the V, 86% of the Pb, 89% of the Co, and 80% of the W from seawater solutions with initial concentrations of 0.1 to 10 ppm metal.

Although the adsorption of metals on hydrous ferric oxides has been investigated (4,5), the experimental data exist mainly for simple, carefully controlled systems designed to allow for maximum insight into the process of adsorption at the microscopic level. Isotherms were generated for one metal adsorbing on a crystalline hydrous ferric oxide surface in the presence of an inert background electrolyte, usually at low ionic strength. Adsorption in seawater, on the other hand, involves many adsorbing metals adsorbing onto an ill-defined, possibly largely amorphous surface in the presence of a complex background electrolyte at high ionic strength. Any or all of these factors may make it unfeasible to extrapolate data from the simpler systems to seawater.

Factors Which May Affect Adsorption of Trace Metals by Hydrous Ferric Oxide in Seawater

The Nature of the Hydrous Ferric Oxide--

In a study of the effects of ionic strength, temperature and Fe(III) concentration on the hydrolysis and precipitation of ferric oxides from ferric nitrate solution, Dousma and deBruyn (6) found that 6.25×10^{-3}M Fe(III) at 24°C produced an amorphous ferric oxide. Higher temperature and Fe(III) concentration were necessary to produce geothite (α FeOOH). This effect of

temperature had earlier been reported by Kolthoff and Moscovitz (7) who also noted that the surface area of the crystalline oxide was smaller than that of the amorphous oxide and that the former adsorbed three to four times less copper than the latter.

In general, slow hydrolysis and/or elevated temperature are required to produce the crystalline ferric oxides. Hematite (Fe_2O_3) is usually prepared by boiling solutions of ferric nitrate at low pH under reflux for 18 days (8). Goethite is obtained by aging a solution of ferric nitrate at pH 12 for 24 hours at 60° (9). These methods produce particles of considerable uniformity in size and shape whose composition depend most strongly on the pH and the anion present in the solution.

Gadde and Laitinen (10) prepared amorphous hydrous ferric oxide by adjusting the pH of a 0.1M ferric nitrate solution to 6 and allowing the precipitate to settle for 2 hours at room temperature. After filtering, washing and aging overnight in distilled water at pH 6, the suspension was used for the experiments. X-ray powder diffraction confirmed that the oxide was amorphous.

Matijevic reports that the background anions, although responsible for the particle characteristics, are not found in the solid phase. Ellis et al. (11), on the other hand, found that Cl^- ion is specifically adsorbed by β FeOOH and cannot be removed completely even with extensive washing with distilled water or by ion exchange.

An extensive investigation of the slow hydrolysis of partially neutralized Fe(III) solutions in the nitrate, chloride and perchlorate solutions was carried out by Murphy, Posner and Quirk (12). They found that the initial polymerization process yields spherical polycations independent of the anion present. The anion does affect the subsequent aging and crystalline structure of the precipitate as it progresses from the spherical polycations to rods to rafts. Rods are formed from linear coalescence of spherical polycations and addition of unpolymerized ferric species in solution. Both rods and spherical polycations are X-ray amorphous. Rafts result from lateral coalescence of rods and show the X-ray pattern of geothite or β FeOOH.

In nitrate and perchlorate solutions α FeOOH (goethite) predominates, while in chloride solutions β FeOOH is formed. The formation of β FeOOH in chloride solution is thought to arise from the penetration of the Cl^- ion into the polycations resulting in a different internal structure when the polycations coalesce. The Fe(III) concentration does not affect the crystalline structure in chloride solutions and increased ionic strength only increases the rate of precipitate formation. In more dilute solutions both nitrate and perchlorate preparations also contained traces of γ FeOOH (lepidocrocite). High ionic strength or anion affinity for the Fe^{3+} ion inhibit the formation of this crystalline form.

In a study of Fe(III) speciation in seawater, Byrne and Kester (13) note that the X-ray amorphous solid phase formed initially in solutions supersaturated with respect to $Fe(OH)_3$ is slowly transformed to a more stable crystalline solid phase. This transformation is extremely slow, however, and after

several months of aging a substantial portion of the solid phase still exists as the amorphous oxide. Dousma and deBruyn had also noted this slow transformation, but found that when the X-ray amorphous solid initially formed in nitrate solution was studied by infrared techniques, the presence of α FeOOH (geothite) was suggested. It has been proposed that the iron oxide found in seawater, while X-ray amorphous, actually has a largely geothite nature (14).

The ferric oxide in seawater may have originated from terrestrial sources or may have been precipitated *in situ*. Since an *in situ* precipitation would occur in the presence of the potentially adsorbing trace metals, the question is raised whether coprecipitation will be the same as adsorption on a previously formed surface. Kolthoff and Moskovitz (7) found that if the oxide was formed at room temperature (amorphous), there was only a slight increase in the amount of copper coprecipitated versus copper adsorbed. With precipitate formed at 98°C, however (crystalline), the differences were more pronounced. Kurbatov, Kulp and Mack (15) found that a higher percentage of strontium and barium was coprecipitated than was adsorbed on an amorphous oxide, but that after several days of standing at pH 8 the amounts of adsorbed and coprecipitated metal were identical. Gadde and Laitinen (10) found that more lead was adsorbed on hydrous ferric oxide if it was present in the solution during the precipitation than if it was added immediately after the precipitation. Aged hydrous ferric oxide adsorbed less lead than fresh, and lead adsorbed on the aged oxide was more efficiently recovered, suggesting that some occlusion occurs in the coprecipitation process. In a later paper, however (16), under the same conditions they report that the effect of aging of the hydrous ferric oxide, either in the presence of lead or before it was added, on the amount of lead adsorbed was not pronounced.

The Complexity of the Background Electrolyte--

The inert background electrolyte used in adsorption experiments usually consists of a dilute solution of a simple salt whose ions have no specific chemical interaction with the surface. Seawater is a complex solution which contains high concentrations of the divalent ions Ca^{2+} and Mg^{2+} which may specifically adsorb on the hydrous ferric oxide and out-compete a less concentrated trace metal for the available surface sites. Alternatively, ligands such as Cl^- that form stable complexes with the adsorbable metal may outcompete the surface for the metal. In either case, a reduction in adsorption of trace metal would be expected.

McNaughton and James (17) reported no exchange or competition between Na^+ or Mg^{2+} and the hydrolyzed Hg(II) species adsorbed on αQuartz. On the other hand, O'Connor and Kester (18) found that Mg in a concentration equal to that in seawater suppresses Co^{2+} adsorption onto illite, but not Cu^{2+} adsorption. It is possible that adsorption on the clay, illite, and the oxide αQuartz occur through different mechanisms and that results from one surface are not relevant to the other.

The effect of competing ligands has been interpreted in several different ways. Forbes, Posner and Quirk (4) interpreted the failure of $HgCl_2$ to adsorb on goethite as an indication that coordinated hydroxyl groups play a vital role in adsorption. The same reasoning was used by McNaughton and James to explain the same result for $HgCl_2$ on αQuartz. They had found that the abrupt

authors have expressed doubt as to the applicability of this method to adsorption on hydrous oxides.

There is no reason to expect that adsorption of a gas occurs via the same mechanism as specific chemical adsorption of ions from solution. In addition, removing the solid from suspension and drying it in order to perform a BET determination may drastically affect the physical configuration of the solid and alter the surface.

Another technique which is sometimes used involves the adsorption of a dye, such as wooly violet, followed by removal of the solid from the suspension and colorimetric measurement of the residual dye in solution. Again the adsorption of large dye molecules is not necessarily the same as adsorption of metal cations, but this technique can be used on an aqueous suspension of the solid.

When the surface charge is attributed to specific sites on the surface, the available reaction sites may be determined by acid-base titration of the surface. This assumes that all sites which react with acid and base will also react with adsorbing metals.

Regardless of the physical picture of surface charge distribution, the determination of the available surface on an amorphous hydrous ferric oxide suspended in the medium in which it was precipitated is difficult to carry out. B.E.T. determinations cannot be made on solution; dye methods, while feasible, are not likely to be appropriate; and acid-base titrations are difficult to interpret because of the unknown concentration of strong acid or base already present in the suspension after precipitation of the oxide.

If the available surface is limited, it should be possible to demonstrate that the amount of metal adsorbed on a given amount of oxide reaches a limiting or plateau level above which an increase in the equilibrium concentration of the metal does not result in further adsorption. James and Healy (21) found that for Co^{2+} adsorption on SiO_2, isotherms plotted as adsorbed Co^{2+} versus free Co^{2+} did not reach a plateau as such. With increasing Co^{2+} the isotherms converged toward the region where free Co^{2+} concentration was limited by the solubility of $Co(OH)_2$. They estimated a maximum adsorption density corresponding to bare Co^{2+} ions being separated by two to four water molecules.

It was pointed out by James (25), however, that the adsorption and precipitation processes are apparently independent since a smaller percent of the total Co^{2+} is adsorbed with increasing added metal, which is opposite to the concentration dependence of precipitation and polymerization.

Further evidence that adsorption and precipitation are independent processes is found in very early work by Kurbatov (26) on the preparation of "highly emanating preparates". These are preparations of hydrous ferric oxide containing adsorbed Ra used to obtain nuclear emanation in exactly measured quantities. He found that exceeding the Ksp of Ra or Ba salts resulted in preparates of diminished radioactivity. This was attributed to the formation of microscopic crystals of the salts which resulted in less Ra

rise in the isotherm for Hg(II) adsorption on αQuartz corresponded to the pH at which $Hg(OH)_2$ predominates in the speciation diagram. The correlation between adsorption and hydrolysis led Matijevic (20) to the conclusion that the hydroxyl group is responsible for the adsorption of ions on colloid particles. He postulated that hydrogen bonding may play a decisive role.

James and Healy (21) rejected the idea that adsorption and hydrolysis were related because of the presence of the -OH group. Instead, they suggested that in lowering the charge on the central cation, hydrolysis made it easier to disrupt the secondary hydration sheath of the metal cation because the charge dipole interactions were weakened. The disruption of the secondary hydration sheath is necessary if an adsorbing cation is to move to within one water molecule of the surface, their definition of specific adsorption. To test James and Healy's interpretation of the correlation between hydrolysis and adsorption, Stanton and Burger (22) used acetate and phosphate ions to reduce the charge of Zn^{2+}. Acetate had little effect, but phosphate enhanced the adsorption of Zn^{2+} on amorphous iron and aluminum oxides. They interpreted the different results for the two anions as indicative of bridging between the zinc ions and the oxide surface by the phosphate ions, similar to the bridging role played by hydroxyl ions. Acetate could not form oxo bridges, so had no effect.

In ammoniacal media, Kolthoff and Moskovitz (7) found that increased NH_4^+ concentration decreased Cu^{2+} adsorption on hydrous ferric oxide and attributed it to lowering of the OH^- concentration by the NH_4^+. Increased NH_3 concentration, while increasing OH^- concentration, also reduced Cu^{2+} adsorption, however. This effect was due to the formation of the stable Cu^{2+} -NH_3 complexes which apparently did not adsorb.

With illite, O'Connor and Kester (18) found less copper adsorbed at a given pH from seawater or 0.7M NaCl than from an artificial river water solution. There was no difference if the system was CO_2 free or contained a carbonate buffering system, however. Vuceta (23) also found that a carbonate buffering system neither enhanced nor depressed adsorption of Cu^{2+} and Pb^{2+} on αQuartz. In both cases the HCO_3^- concentrations were in the range of the concentration in natural waters and the CO_2 was atmospheric. Under these conditions, the carbonate complexes of the metals are not the predominant species.

The Presence of Many Potentially Adsorbing Trace Metals and Limited Surface for Adsorption

Much of the existing data for adsorption of metals on hydrous oxides has been obtained with an excess of adsorbing surface and one metal in solution. The meaning of available surface is not clear and has been measured or defined by various methods.

If the charge on the surface is pictured as evenly distributed over the entire surface area, it is common to assume that the limit of adsorption density is surface monolayer coverage. This value is usually obtained by measuring available surface area per amount of solid with the B.E.T. gas adsorption method (24) or a similar technique. Then from calculations based on hydrated ionic radii, a maximum adsorption density is obtained. Various

or Ba being uniformly distributed throughout the hydroxide.

Gadde and Laitinen (16) were able to demonstrate a plateau value for Pb^{2+} adsorption on amorphous hydrous ferric oxide at pH 6. Their value was 0.28 moles Pb^{2+} per mole of Fe(III). They could not demonstrate a plateau at pH 5 or for Pb^{2+} on hydrous manganese oxide. Cd^{2+}, Zn^{2+} and Th^{2+} reached a limiting plateau on amorphous hydrous manganese oxide at about 0.2 mole/mole Mn at pH 6. The values for the plateau levels were found to be pH-dependent, decreasing with decreasing pH.

With a hematite suspension, Breeuwsma and Lyklema (27) found that Ca^{2+}, Mg^{2+}, Sr^{2+}, and Ba^{2+} were specifically adsorbed and shifted the pH of the suspension toward lower pH until it reached pH 6.5 in 10^{-3}N salt solution. No further shift was observed up to 10^{-1}N salt solution, indicating no further adsorption. The surface charge computed from maximum adsorption density was lower than 1 micro coulomb per cm^2. Comparison of this value with the computed maximum surface charge obtained from potentiometric titration and B.E.T. surface area data of 75 $\mu C\ cm^{-2}$, indicates the presence of special groups or adsorption sites on the surface.

The fact that a hydrous oxide surface can be saturated opens the possibility of competition between adsorbing metals as the total metal concentration exceeds the concentration of available sites. Gadde and Laitinen (16) were able to demonstrate that Pb^{2+} outcompetes Cd^{2+}, Zn^{2+}, and Th^{2+} for hydrous manganese oxide sites regardless of which metal is added first. This demonstrates not only competition but the existence of a reversible adsorption mechanism through which an adsorbed metal ion can be replaced by other competing metal ions. On hydrous ferric oxide, Zn^{2+}, Ca^{2+}, and K^{+} all in large excess over Pb^{2+} had no effect on the Pb^{2+} adsorption.

Kurbatov, Kulp and Mack (28) in a study of Ba and Sr adsorption on hydrous ferric oxide found plateaux for both metals at about 10^{-2} mole of metal per mole of ferric oxide, but could demonstrate competition only if one metal was present in great excess over the other.

Theoretical Models of Adsorption

Predicting the possible effects of each of these factors on the adsorption isotherms on hydrous ferric oxide in seawater depends to a great extent on the physical and chemical picture of adsorption that is considered. The basic concepts on which most adsorption models have been built were expounded in the Gouy-Chapman theory of the electrical double layer as modified by Stern -Grahame. This theory, known as the electrical double layer or EDL theory, was derived with reference to either mercury drops which become charged as the result of the external application of a known potential difference, or solids such as AgI which become charged as the result of assymetrical dissolution of the lattice ions and for which these ions are potential determining. The double layer potential for these solids is gotten from the Nernst Equation:

$$\Psi_o = \frac{RT}{F} \ln \frac{a_+}{a^o_+} \qquad (1)$$

where Ψ_o = the potential difference across the electrical double layer formed by the reversible transfer of potential determining ions

R = the gas constant

T = the temperature in ^oK

F = the Faraday constant

a_+ = the activity of the positively charged potential determining ion in solution

a^o_+ = the activity of the positively charged potential determining ion at the point of zero charge

For either surface, rigorous thermodynamic calculations relating the surface charge and the potential of the electrical double layer are possible. The adsorption of ions at either of these surfaces is a function of the coulombic attraction or repulsion of the charged surface for the ions and a specific chemical interaction energy.

$$\Delta G_{ads} = ZF\Psi_\delta - \Phi \tag{2}$$

where Z = the charge on the adsorbing ion

F = the Faraday constant

Ψ_δ = the potential at the distance of closest approach of the adsorbing ions (δ)

Φ = the specific chemical interaction energy

The physical picture of adsorption that results from this treatment is represented in Figure 1.

Application of EDL theory to hydrous oxides is not completely straightforward. With hydrous oxides, much higher surface charges are developed than can be accounted for by the electrokinetically measured double layer potentials (zeta potentials). The surface charge arises from reaction of the surface with H^+ and OH^- ions, which are therefore the potential-determining ions for oxides.

$$\begin{aligned} \equiv M\text{-}OH + H^+ &\rightarrow \equiv M\text{-}OH_2^+ \\ \equiv M\text{-}OH + OH^- &\rightarrow \equiv M\text{-}O^- + H_2O \end{aligned} \tag{3}$$

The Nernst equation for oxide surfaces takes the form:

$$\Psi_o = 2.3 \frac{RT}{F} (pH_{PZC} - pH) \tag{4}$$

where pH_{PZC} = the pH at which the surface contains equal numbers of adsorbed H^+ and OH^- ions

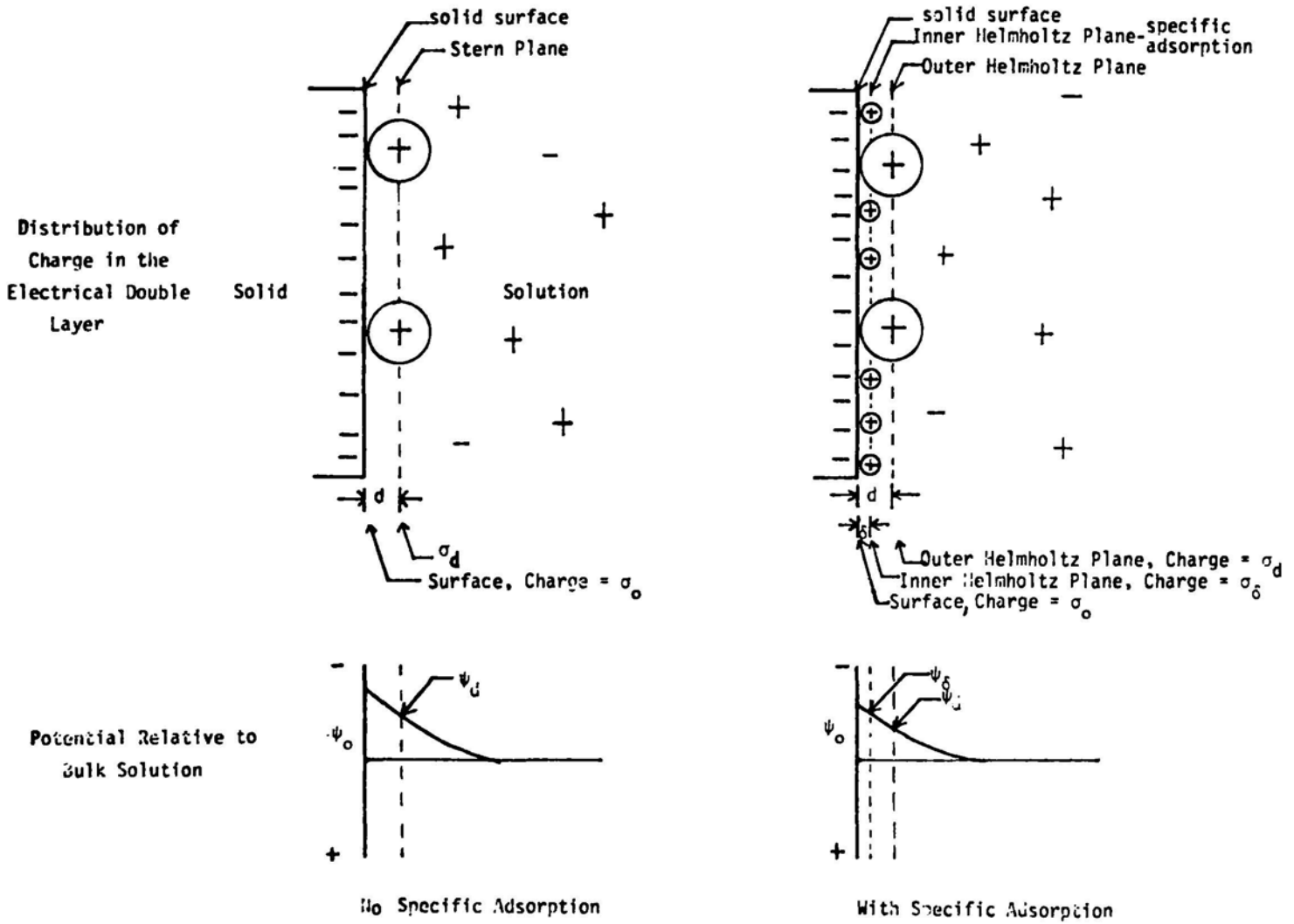

Figure 1. Adsorption in the electrical double layer.

pH = any other pH

The use of the Nernst equation to calculate double layer potentials for oxides is only considered valid near pH_{PZC} where the number of adsorbed potential determining ions is small compared to the number of surface lattice ions. Lyklema (29) points out that in order for equation (4) to hold, the chemical potential of H^+ on the surface, $^{S}H^+$ must be assumed to be independent of the activity of H^+ on the surface. He maintains that this is unlikely since H^+ is not a constituent of the unhydrated solid, and thus adsorption of H^+ will cause the surface layer composition to be different from that of the bulk solid.

This problem is also discussed by Berube and deBruyn (30) who observed that the differential capacity of the double layer on hydrous oxides, given by:

$$C = \frac{\partial \sigma_o}{\partial \Psi_o} \tag{5}$$

where σ_o = surface charge

Ψ_o = surface potential relative to the bulk solution

is much larger than the differential capacities for mercury or silver iodide surfaces.

Several models of the double layer on hydrous oxides which could account for the existence of high surface charge despite low double layer potential have been proposed. The porous double layer model of Breeuwsma and Lyklema (31) is based on the ability of the potential determining ions and some counter ions to penetrate into the surface layers of the solid. Thus the specificity of a charged surfaced in adsorbing ions of the opposite charge depends on the geometric penetrability of the ions as well as on their affinity for the solid. Their data suggests that of the two, porosity is the more important factor. Since much of the surface charge would be neutralized within the pores of the solid, the potential across the electrical double layer would be lower than that expected from consideration of the total surface charge.

Berube and deBruyn in their structured water model place the locus of the potential determining H^+ and OH^- ions not on the surface itself, but in a layer at least one molecular layer of water away. This highly structured water layer between the surface and the adsorbed potential determining ions is dissociated, possibly to a greater extent than bulk water, because of its chemisorption at the surface. Since H^+ and OH^- are now lattice ions, the constraints on the Nernst equation are no longer a problem. Adsorbed counterions, especially strongly hydrated ones, can now approach the region occupied by the surface charge very closely, again allowing high surface charges to exist despite low potentials some distance from the surface.

In the site-binding model of Yates, Levine and Healy (32), the charged

surface sites arising from reaction of the surface with potential determining ions, react further with ions of the indifferent (non-specifically adsorbed) supporting electrolyte, e.g. NaCl.

$$\equiv M\text{-}OH_2^+ + Cl^- \rightleftarrows \equiv M\text{-}OH_2Cl$$
$$\equiv M\text{-}O^- + Na^+ \rightleftarrows \equiv M\text{-}O\text{-}Na \qquad (6)$$

All sites involving the potential determining H^+ and OH^- ions are in one plane at potential Ψ_o. The supporting electrolyte ions are situated in a different common plane, the Inner Helmholtz Plane. The Outer Helmholtz Plane is the plane of closest approach of ions in the diffuse part of the double layer. Again high surface charge and differential capacity of the double layer can exist despite low potential at the Outer Helmholtz Plane.

These models have been proposed to explain characteristics of the electrical double layer peculiar to hydrous oxide surfaces. They produce refinements in the isotherms for electrostatically bound adsorbants, but do nothing to elucidate the nature of specific chemical adsorption. The fact that charge-reversal due to super-equivalent adsorption of cations on a negatively charged surface and the adsorption of cations on a positively charged surfaces exist, indicates that in many cases the specific chemical interaction is more important than the electrostatic interaction.

James and Healy modified the EDL treatment of adsorption by adding a third energy term to equation (2). They observe that for each metal specifically adsorbing on a given surface there is a critical pH range, usually less than two units wide, over which the fractional amount of metal adsorbed increases from zero to almost unity. The onset of the range is related to the onset of hydrolysis and the subsequent lowering of the charge of the adsorbing ion. The added term opposes adsorption of highly charged free aquo metal ions and decreases in magnitude as the charge on the metal decreases with hydrolysis. Thus:

$$\Delta G^o_{ads} = \Delta G^o_{coul} + \Delta G^o_{chem} + \Delta G^o_{sol} \qquad (7)$$

ΔG^o solvation represents the energy required to disrupt the hydration sheath of an adsorbing metal ion so that it can move to within one water molecule of the surface. It depends on the dielectric constant of the adsorbant and the charge and radius of the adsorbing metal ion. The more hydrolyzed the adsorbing metal ion is, the less charged it is and the less unfavorable the energy of solvation is because the water of hydration is less tightly bound. This model represents a departure from the classical EDL treatment of adsorption in that it includes more information about the nature of the specific chemical adsorption process.

A different approach to adsorption on oxides is taken in the surface complexation model (33). Adsorption is treated as a chemical reaction whose equilibrium constants are affected by the presence of the charged surface. First, since the development of the surface charge is dependent on the acid-base properties of the oxide, one can write the constants for the surface

reactions:

$$\equiv M\text{-}OH_2^+ \rightarrow \equiv M\text{-}OH + H^+ \quad ; \quad Ka_1 = \frac{\{\equiv M\text{-}OH\}[H^+]}{\{\equiv M\text{-}OH_2^+\}}$$

$$\equiv M\text{-}OH \rightarrow \equiv M\text{-}O^- + H^+ \quad ; \quad Ka_2 = \frac{\{\equiv M\text{-}O^-\}[H^+]}{\{\equiv M\text{-}OH\}} \tag{8}$$

where { } indicates surface groups

[ ] indicates species in solution

These constants can be evaluated experimentally from data for the potentiometric acid-base titration of the surface. The constants obtained in this manner are "microscopic" constants, however, which are pH dependent. The "microscopic" constants are analogous to the series of acidity constants obtained as protons are removed from proteins or other polymers. As each successive proton is removed, the remaining protons become more tightly bound because of the increasing number of negatively charged groups. Likewise, for a charged surface, the acidity of a proton depends on the relative charge on the rest of the surface which in turn depends on the pH. These microscopic or apparent acidity constants can be converted to intrinsic constants, independent of pH, by extrapolating the apparent constant versus surface charge curve to the zero charge condition. From EDL theory it follows that the change in the acidity constants with surface charge is given by:

$$K_a = K_{a_{int}} \exp\{F\Psi/RT\} \tag{9}$$

where $K_{a_{int}}$ = intrinsic acidity constant

K_a = microscopic or apparent acidity constant

Similarly, for a specifically adsorbed metal ion (Me^{2+}), the surface reactions and stability constants are given by:

$$\equiv M\text{-}OH + Me^{2+} \rightarrow \equiv M\text{-}O\text{-}Me^+ + H^+ \quad ; \quad K_1^s = \frac{\{\equiv M\text{-}O\text{-}Me^+\}[H^+]}{\{\equiv M\text{-}OH\}[Me^{2+}]}$$

$$2\equiv M\text{-}OH + Me^{2+} \rightarrow (\equiv M\text{-}O)_2Me + 2H^+ \quad ; \quad \beta_2^* = \frac{\{(\equiv M\text{-}O)_2Me\}[H^+]^2}{\{\equiv M\text{-}OH\}^2[Me^{2+}]} \tag{10}$$

for mono and bidentate complexes. Again, these are microscopic constants and can be extrapolated to the pH of zero charge to obtain the intrinsic constants.

This model presents adsorption as a chemical reactions which is influenced by electrostatic interactions. It does not give any direct insight into the electrical properties of the surface or address itself to purely coulombic interactions.

In order to determine what are the effects of the various factors discussed above on the adsorption of trace metals by hydrous ferric oxide in seawater, it is first necessary to isolate the factors. This can be done by starting with a simple system of one metal, for example Cu^{2+}, adsorbing on hydrous ferric oxide in a simple, non-specifically adsorbed background electrolyte, for example $NaClO_4$. Once a baseline result is established for the simple system, the system can gradually be changed and/or made more complex and any changes in the adsorption isotherms can be ascribed to the appropriate factor. Finally, the isotherm for Cu^{2+} on hydrous ferric oxide in the presence of the other adsorbable metals in seawater can be interpreted on the basis of the known influence of each of the factors. Using the experimental results, it should be possible to determine which, if any, of the theoretical models of adsorption provides a satisfactory explanation for the process of adsorption in seawater.

SECTION 2

EXPERIMENTAL MATERIALS AND METHODS

MATERIALS

Chemicals

All reagents were prepared from Analytical Reagent grade chemicals using distilled, deionized water.

Sodium hydroxide solutions were prepared from 50% NaOH solution and standardized against potassium acid phthalate with phenolphthalein indicator. They were stored in polyethylene dispenser bottles and kept CO_2 free.

6 N hydrochloric acid was distilled from a quartz still. Solutions were standardized against standard base with phenolphthalein indicator.

Synthetic Ocean Water (S.O.W.) was prepared according to the formulation of the FWPCA (34). This is a complex solution of eleven salts containing the major constituents of seawater. The composition is given in Table I. The S.O.W. was passed through a Chelex 100 chelating resin column at pH 8.5 to remove trace metals present as impurities in the reagent grade major salts (35).

Copper and lead stock solutions were 0.01 and 0.1M $Cu(NO_3)_2$ and $Pb(NO_3)_2$. 50 µl of the appropriate 0.01 M solution was added to 50 ml of sample gave a final trace metal concentration of 1×10^{-5}M. This concentration was used for most experiments with 1×10^{-4}M (as Fe) hydrous ferric oxide. In the experiments where total trace metal concentration was varied, differing amounts of the stock solutions in both concentrations were used to give the desired final concentration. Stock solutions were naturally acidic as a result of the hydrolysis of the Cu^{2+} and Pb^{2+}. Periodically fresh stock solutions were prepared and both old and fresh solutions were analyzed by Atomic Absorption Spectrophotometry. Results showed that the stock solutions remained stable indefinitely.

The ferric iron stock solution was 1.0 M $Fe(NO_3)_3$. It had a pH of 2.7 immediately after preparation, so no acid was added to stabilize it. The amber color of this solution increased in intensity with time, indicating increasing polymerization of the iron hydrolysis species, but no cloudiness or precipitate appeared. Periodic iron analysis by the orthophenanthroline procedure indicated that the concentration was stable indefinitely.

Other trace metal solutions were prepared fresh as needed from reagent

Table 1

The Composition of S.O.W.

salt	final concentration
NaCl	4.20×10^{-1}M
$CaCl_2$	1.05×10^{-2}M
KBr	8.40×10^{-4}M
NaF	7.14×10^{-5}M
KCl	9.39×10^{-3}M
H_3BO_3	4.85×10^{-4}M
Na_2SO_4	2.88×10^{-2}M
$NaHCO_3$	2.38×10^{-3}M
$SrCl_2$	6.38×10^{-5}M
$MgCl_2$	5.46×10^{-2}M

grade chemicals.

Apparatus

Before use, all glassware was cleaned, rinsed with distilled, deionized water, soaked in 3N HCL for at least 12 hours, and rinsed with distilled, deionized water. All tubing and stirrers which contacted the sample solutions were Teflon. Some experiments were done in acid-soaked glass beakers, others in Teflon beakers. The apparatus used for most of the experiments is shown in Figure 2. The sample was placed in a 100 ml beaker, either glass or Teflon with a Teflon coated stirring bar. This beaker was placed inside a 250 ml jacketed glass beaker which was connected to a Haake circulating constant temperature bath. The temperature was maintained at 25°C for all experiments. A #10 silicone rubber stopper bored to accommodate two electrodes, a N_2 inlet tube, a sample withdrawal tube and a reagent introduction inlet fit snugly into the top of the beaker. The N_2 was passed first through an Ascarite-filled drying tube to remove CO_2 and then through distilled, deionized water to saturate it before it entered the reaction vessel through Teflon tubing. The sample withdrawal tube was a Teflon tube ending in a Luer-loc fitting. This end was kept immersed in a test tube of water to provide a pressure outlet without allowing air to enter the system. The other end was only immersed in the sample when an aliquot was being withdrawn. Reagents were introduced into the system with Eppendorf pipettes. The reagent introduction inlet was an Eppendorf pipette tip (5-100 µl size), with about 2 cm cut off from the tip inserted in the stopper until the cut off end was flush with the stopper bottom. Except when in use, this inlet was stopped with another Eppendorf pipette tip either filled with Ascarite or closed off with a medicine dropper bulb. When completely assembled this apparatus was a CO_2-free system. The pH was measured with an Orion Model 91-01 glass electrode versus an Orion Model 90-02 double junction reference electrode. The electrodes were calibrated daily using Fisher Certified Buffer Solutions at pH 7 and 4. Readout was obtained on either an Orion Model 701 digital pH meter of an Orion Model 801A digital ionalyzer. The output was recorded on a Cole-Parmer dual channel strip chart recorder.

METHODS

Preparation of Hydrous Ferric Oxide

The hydrous ferric oxide sols used for these experiments were prepared by filling a volumetric flask with the appropriate background electrolyte solution, stirring with a magnetic stirring bar, and adding stock 1M $Fe(NO_3)_3$ with an Eppendorf pipette. In $NaClO_4$ and NaCl solutions a stoichiometric amount of 1N NaOH, calculated by assuming the formula $Fe(OH)_3$ for the precipitate, was added to raise the pH and ensure complete, fast precipitation. In synthetic ocean water (S.O.W.), the natural buffering made this unnecessary, as the pH stayed around 7.5. All preparations were done open to the atmosphere. For experiments using freshly precipitated hydrous ferric oxide (HFO), only enough suspension was prepared for one day's experiments, usually 100 or 250 ml. For experiments with aged HFO, 2 liters were prepared, which yielded forty 50 ml samples.

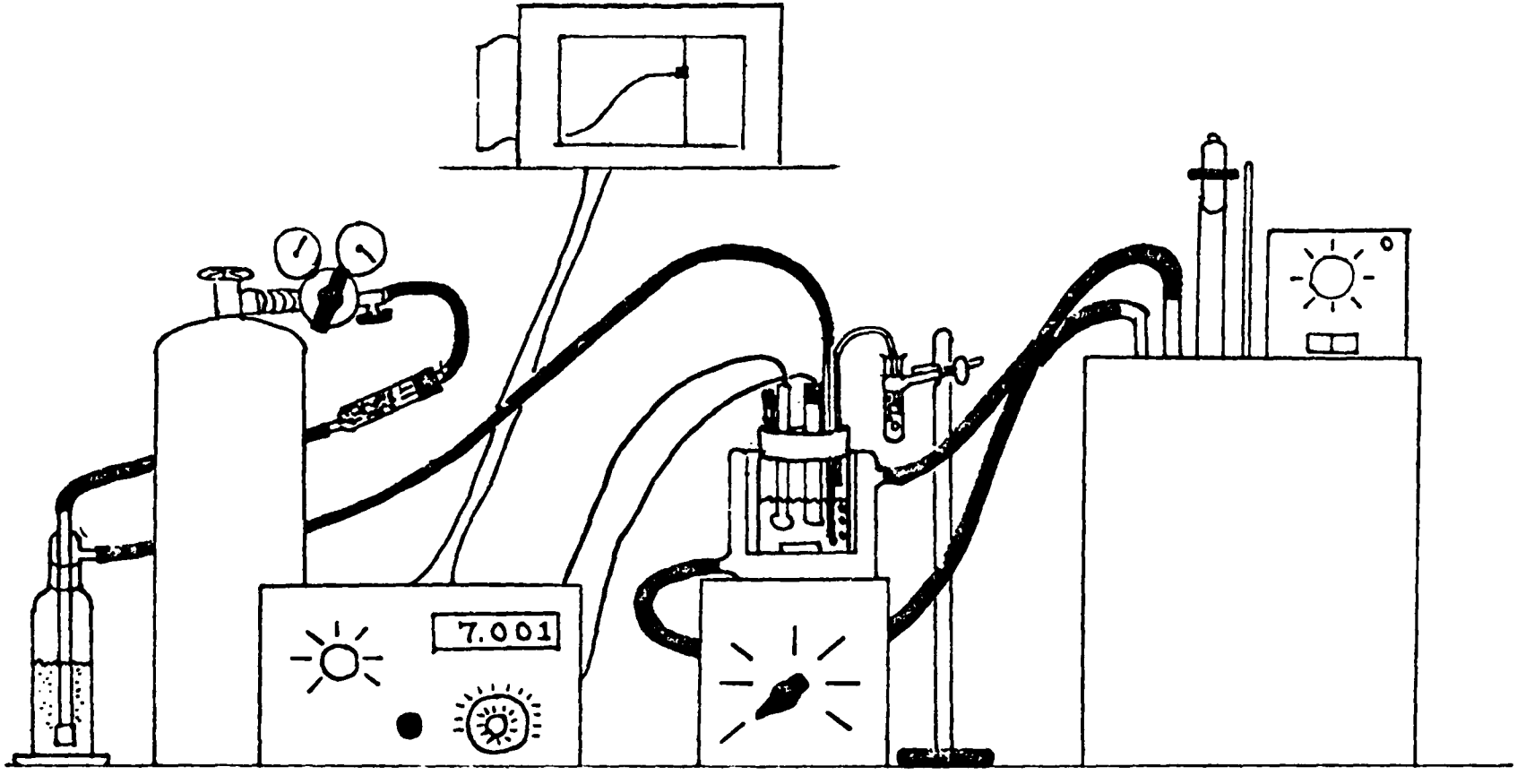

Figure 2. Experimental apparatus.

In experiments done on "fresh" precipitates, the suspension was stirred for one hour before sampling. During stirring the oxide remained uniformly suspended and no clumping of particles or accumulation of solid on the walls of the flask occurred. Samples were withdrawn with 50 ml volumetric pipettes while the suspension was stirred vigorously. The sample was transferred to the beaker and placed in the apparatus shown in Figure 2. The experiment was begun after pH equilibrium was reached. A signal drift below 0.002 pH units/min was used as the criterion for equilibrium. The total time elapsed between preparation and the start of an experiment on fresh hydrous iron oxide was around 3 hours.

In the first experiment done on "aged" precipitates, the preparation was stirred continuously and sampled at appropriate times measured as time after preparation. After 144 hours it was noticed that small shavings of Teflon had flaked off the magnetic stirring bar and had become nuclei for agglomerations of the ferric hydroxide sol. This was extensive enough to significantly alter the concentration of iron in the samples withdrawn, since these agglomerates were not taken into the sampling pipettes. Later experiments on aged precipitates were done with sols that were quiescent between samplings and only stirred during sampling. The settling out of the precipitate did not appear to affect its later dispersability or chemical characteristics.

Potentiometric Titrations

The titrations were performed in the CO_2-free system by adding a known excess of acid--either $HClO_4$ for $NaClO_4$ solutions or HCl for NaCl or S.O.W. solutions--to the sample in the beaker, to lower the pH below 4. The N_2 was turned on and the CO_2 purged from the sample. After the pH equilibrated, but not before 10 minutes, the pH was recorded and a known volume of standard 0.05N NaOH (CO_2-free) was added with an Eppendorf pipette. At the low and high ends of the pH range, 50 µl additions were made. At the break, additions were reduced to 10 µl. The pH was allowed to re-equilibrate after each addition and was recorded. A drift of less than 0.002 pH units/min was used as a measure of equilibrium. This was continued until the sample reached pH 10. All titrations were kept free of CO_2.

Generation of Isotherms

To generate an isotherm a 50 ml portion of the hydrous ferric oxide sol was placed in the beaker in the CO_2-free apparatus shown in Figure 2. $HClO_4$ or HCl was added to lower the sample pH below 4 and the sample was purged of CO_2. After pH equilibration a known volume of a trace metal solution was added with an Eppendorf pipette. An addition of 0.05N NaOH (CO_2-free) was made to raise the pH. At low pH, 0.05N NaOH was added in 100 µl portions. Near the break of the titration the size of each addition was lowered to 50, 10, and finally 5 µl. This made it possible to obtain samples distributed over the entire range from pH 4 to pH 7. In the low and high pH regions, pH equilibrations occurred within one minute. Near the break, the time necessary for equilibration became longer, reaching a maximum of about one hour. Equilibration times of longer than one hour were indicative of a clogged reference electrode, a pressure build-up in the system or inadequate stirring. A pH drift back to lower pH indicated CO_2 contamination which

necessitated termination of the experiment.

After pH equilibration the sample withdrawal tube was lowered into the suspension and a 5 cc disposable syringe was attached to the Luer-loc fitting. About 3 ml of the suspension and another addition of base was made to the sample in the beaker. A Swinnex Millipore filter holder with a 0.025 μm Cellulose acetate filter was attached to the syringe containing the withdrawn sample. The sample was expressed through the filter into a 25 ml Erlermeyer flask with a standard taper glass stopper. 10 μl of 6N HCl were added to the flask, it was stoppered, marked for identification and set aside until all samples were collected in the same way.

When all the samples for an isotherm were collected they were analyzed for the metal or metals of interest by flame atomic absorption spectrophotometry.

The efficiency of the 0.025 μm Millipore filters was tested by analyzing the filtrate for iron by the orthophenanthroline procedure. 1.2×10^{-6}M Fe^{3+} was left in the filtrate from a 1×10^{-3}M (as Fe) suspension of hydrous ferric oxide. This corresponds to 99.8% removal of the iron.

Flame Atomic Absorption Spectrophotometry

Flame Atomic Absorption Spectrophotometry was done on a Perkin-Elmer Model 360 double beam atomic absorption spectrophotometer. All of the metals analyzed required an air-acetylene flame. Metal concentrations were always within the detectable range of the instrument so no pre-concentration steps were necessary. Standards were prepared in concentrations to bracket the sample concentrations using the same background electrolyte as the sample. The high salt content of standards and samples caused some variability in absorption values obtained for different aspirations of the same sample. Because of this, all standards and samples were aspirated in random order at least three times. The average of the three values was taken as the absorbance for a sample. The relative standard deviation of the three readings ranged from 1 to 3%. Standard curves prepared from the samples were linear through all points, but had non-zero intercepts on the absorbance (y) axis corresponding to the absorbance reading for background electrolyte with no added metal. It was determined that this was due to the high salt content and its interference with the flame and not to ambient metal concentrations in the reagents by using the Cd lamp to analyze a solution of Cu. Cd has a spectral line at 326.1 nm, very close to the Cu line at 324.8 nm. A distilled water solution of Cu has zero absorbance at this wavelength, but the 0.5 M $NaClO_4$ 0.5M NaCl and S.O.W. solutions all gave absorbance readings corresponding to the non-zero intercept of their standard curves. The non-zero intercept was reproducible and stable from day to day.

SECTION 3

EXPERIMENTAL RESULTS

POTENTIOMETRIC ACID-BASE TITRATIONS

Existing models of adsorption of trace metals by hydrous oxides rely heavily on data from acid-base titrations of the solid. These data are used to compute the pH_{PZC} and the number of reactive sites on the solid surface. In this work, to avoid possible changes in the nature of the precipitate due to filtration, the titrations were performed in the same medium from which the hydrous ferric oxide had been precipitated. Reproducible titrations of the amorphous hydrous ferric oxide used in this work were very difficult to obtain. Similar difficulties were encountered by Davis (36). The experimental errors in the addition of $Fe(NO_3)_3$ and NaOH to the medium resulted in variability in the position of the titration curves. A representative titration curve is shown in Figure 3 for 1×10^{-3}M amorphous hydrous ferric oxide in 0.5 M $NaClO_4$. Similar curves were obtained in 0.1 and 0.25 M $NaClO_4$.

The proton excess or deficiency in the solid phase ($\Gamma_{H^+} - \Gamma_{OH^-}$) is calculated from the titration curves as the difference in the amount of acid or base needed to reach a given pH in the sample and the blank. It is related to surface charge by

$$\sigma_o = \frac{F(\Gamma_{H^+} - \Gamma_{OH^-})}{A} \qquad (1)$$

where σ_o = surface charge

$\Gamma_{H^+} - \Gamma_{OH^-}$ = surface excess H^+ over OH^-

A = surface area

F = Faraday constant

Because the methods available for determining surface area are unsatisfactory for use with suspensions in the medium in which they have been precipitated, surface excess in eq/mole has been substituted for surface charge in this work. If a constant specific surface area is assumed the two differ by only a constant.

Plots of the surface excess shown in Figure 4 for the three ionic strengths are the same within experimental error. They do not exhibit the sigmoid characteristics obtained for other oxides (5, 30, 31). Therefore a

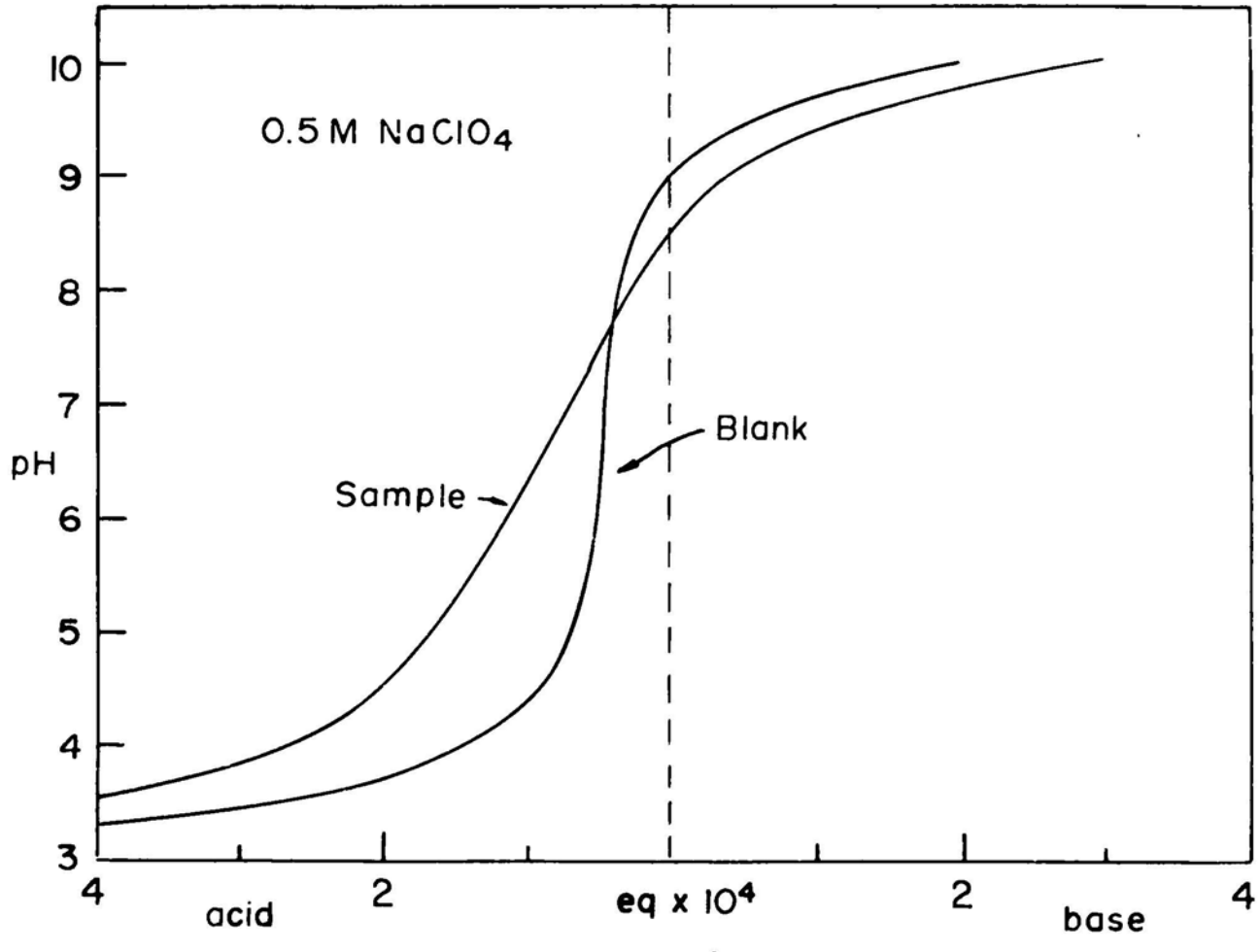

Figure 3. Titration curve for 1 x 10^{-3} M amorphous hydrous ferric oxide in 0.5 M $NaClO_4$.

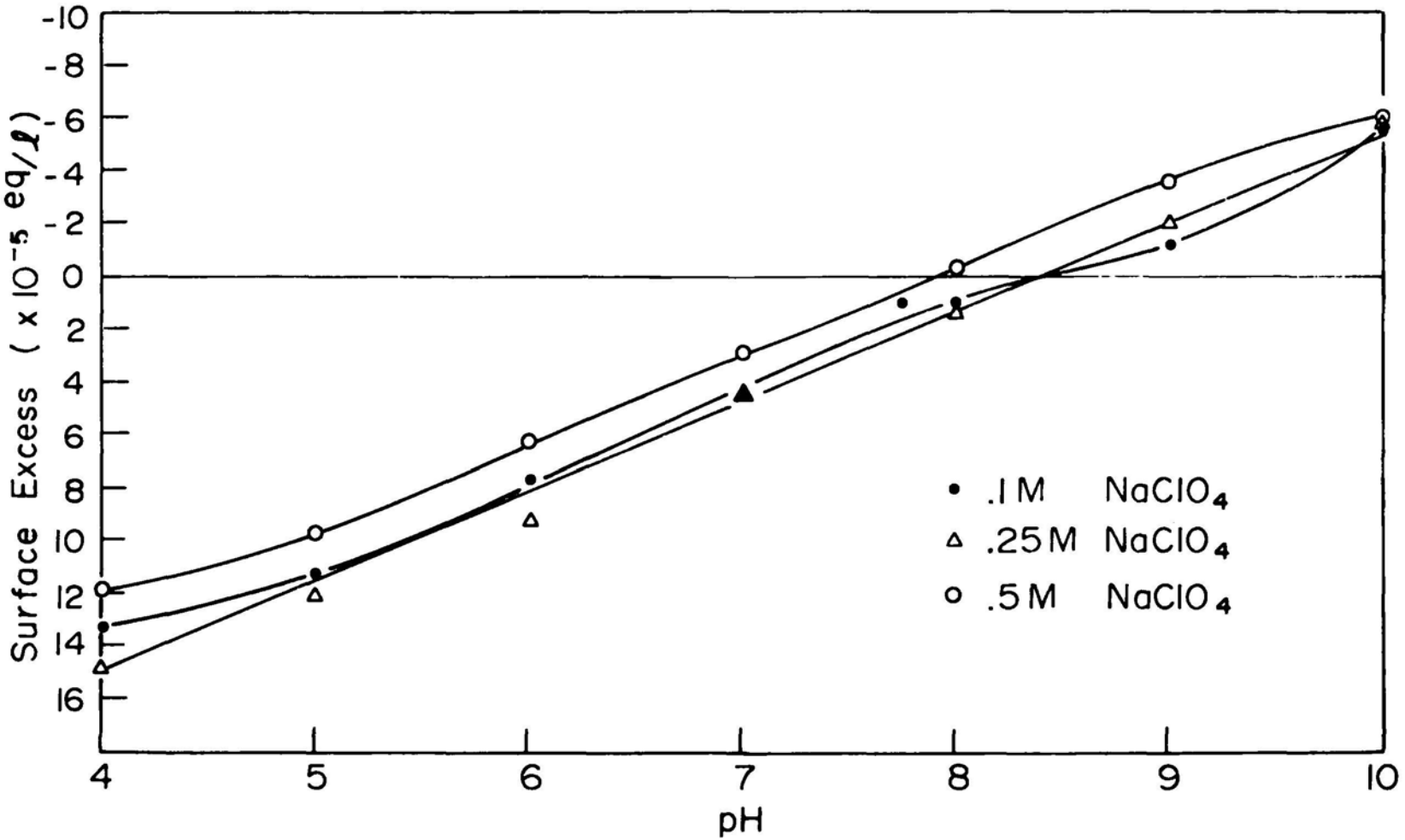

Figure 4. Surface excess H^+ or OH^- as a function of pH for 1 x 10^{-3} M hydrous ferric oxide.

value for maximum reactive sites cannot be obtained, although it must be in excess of 0.15 site/Fe. The pH_{PZC} appears to be in the range of 7.9 - 8.5. This is in agreement with data reported for various crystalline and amorphous iron oxides (4, 5, 8, 29).

Titration curves obtained as soon as possible after preparation of the oxide (ca. 2 hours due to pH equilibration time) required more acid than curves obtained for the same oxide after 24 hours aging. No further change occurred after 24 hours. This shift in the titration curves, shown in Figure 5, can be interpreted as a release of acid or a consumption of base by the aging oxide. The two curves are roughly parallel 1.3×10^{-4} eq apart for 1×10^{-4}M Fe. Copper isotherms obtained simultaneously with the same batch of oxide showed no effect of aging. This is shown in Figure 6 which also illustrates that the same isotherm was obtained when copper was coprecipitated with the iron.

EFFECT OF IONIC STRENGTH

The effect of ionic strength on the Cu^{2+} isotherm was first studied using hydrous ferric oxide precipitated in media of varying ionic strength. The results shown in Figure 7, exhibit a non-systematic variability presumably due to differences among the batches of ferric oxide. To eliminate batch to batch variations in the oxide a large batch of 2×10^{-4}M hydrous ferric oxide was prepared in 0.01 M $NaClO_4$. By appropriate dilution (1:1) with 0.99 M $NaClO_4$, 0.09 M $NaClO_4$, or deionized, distilled water, a background electrolyte concentration of 0.5 M $NaClO_4$, 0.05 M $NaClO_4$ or 0.005 M $NaClO_4$ could be had with the same batch of oxide. As expected, the results were less variable and demonstrate no effect of ionic strength either on the Cu^{2+} isotherm (Figure 8) or on the Pb^{2+} isotherm (Figure 9).

EFFECT OF COMPOSITION OF THE BACKGROUND ELECTROLYTE

The effect of the composition of the background electrolyte was studied in the same way. The Cu^{2+} isotherms obtained with hydrous ferric oxide precipitated in 0.5 M $NaClO_4$, 0.5 M NaCl and S.O.W. (Figure 10) again show a small non-systematic variability. Diluting portions of the large batch of 2×10^{-4}M hydrous ferric oxide in 0.01 M $NaClO_4$ with 2 x S.O.W. and 1.0 M NaCl gave background electrolyte compositions of S.O.W. and 0.5 M NaCl for the same batch of iron. While the Cu^{2+} isotherms were identical to the one obtained in 0.5 M $NaClO_4$ (Figure 11), the Pb^{2+} isotherms were equally depressed relative to the Pb^{2+} isotherm in 0.5 M $NaClO_4$. The difference follows from the relative strengths of the Cl^- complexes of the two metals. While the chloride complexes of Cu(II) are relatively unimportant, Pb(II) is known to form important di and trichloro complexes at $(Cl^-) = 0.5$ M. Apparently the Cl^- complexes are not adsorbed and the result of Cl^- complex formation is a decrease in available Pb^{2+} which depresses the isotherm. Neither the Cu^{2+} nor the Pb^{2+} isotherm is affected by high concentrations of Mg^{2+} and Ca^{2+}, indicating either than Mg^{2+} and Ca^{2+} are not adsorbed or that they can be displaced by Cu^{2+} and Pb^{2+}.

EFFECT OF VARIATION OF METAL AND OXIDE CONCENTRATIONS

An important aspect of the amorphous hydrous ferric oxide system is the

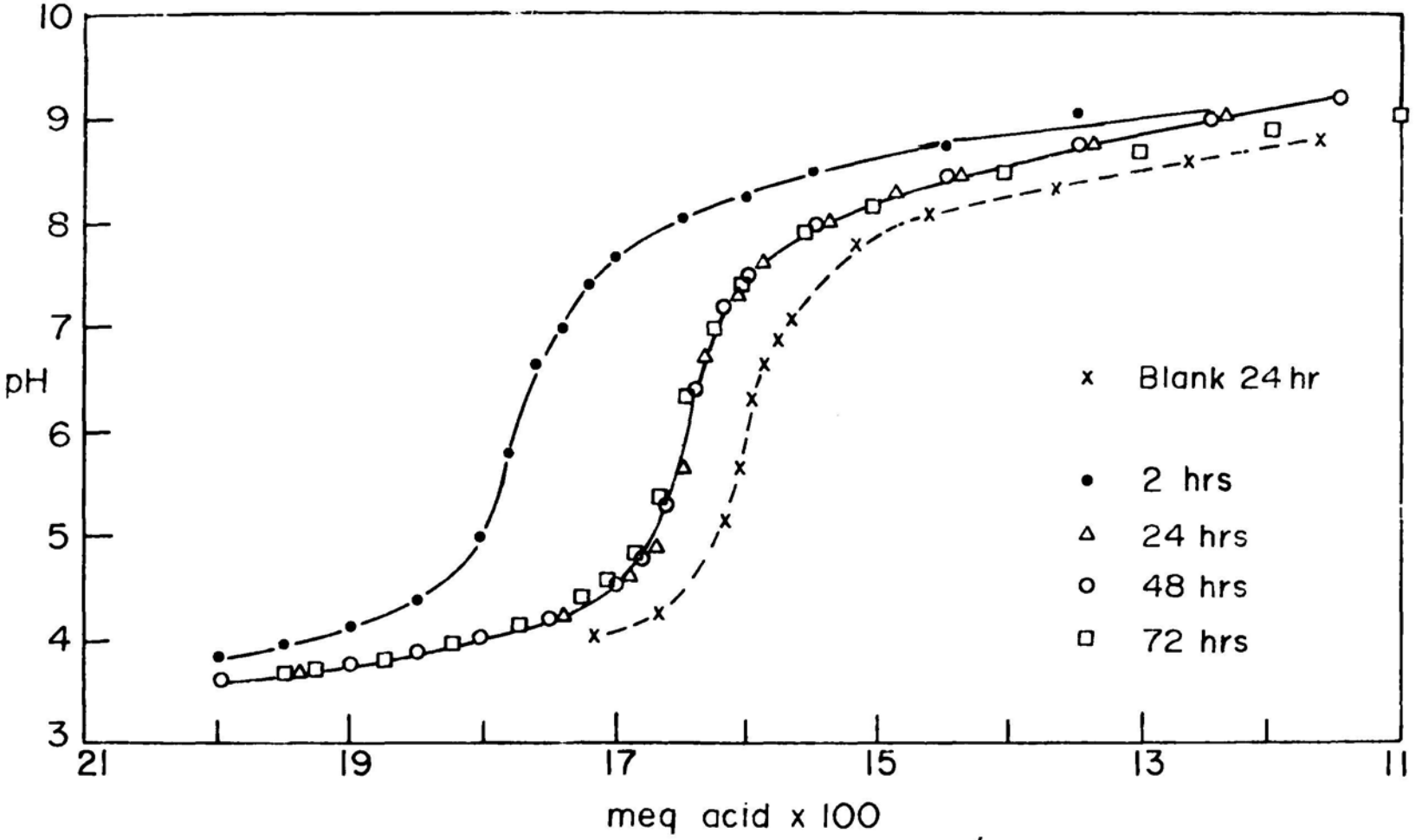

Figure 5. Changes with aging in the titration curve for 1 x 10^{-4}M hydrous ferric oxide in S.O.W.

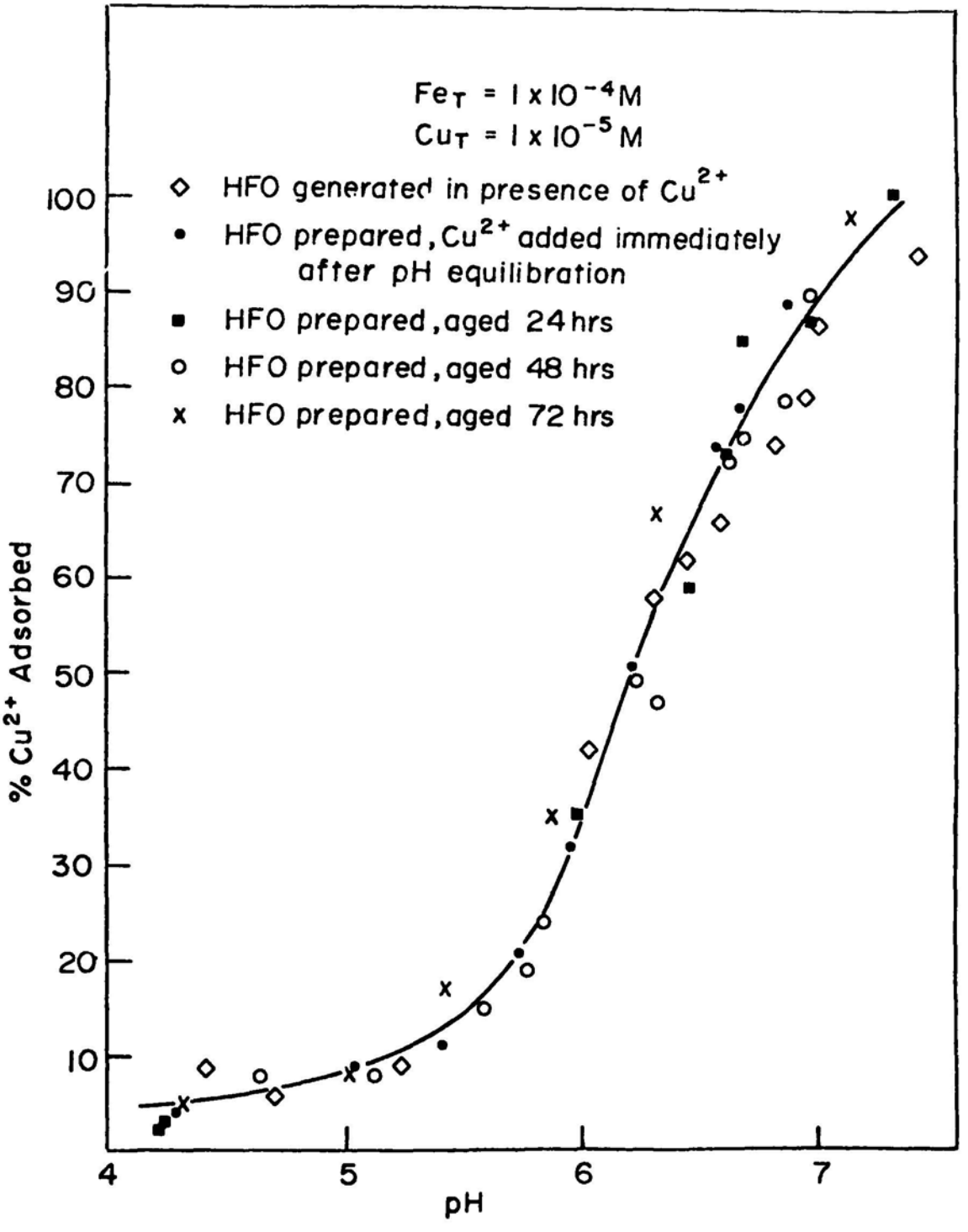

Figure 6. Effect of aging on the Cu^{2+} isotherm for 1×10^{-5}M Cu^{2+} on 1×10^{-4}M hydrous ferric oxide in S.O.W.

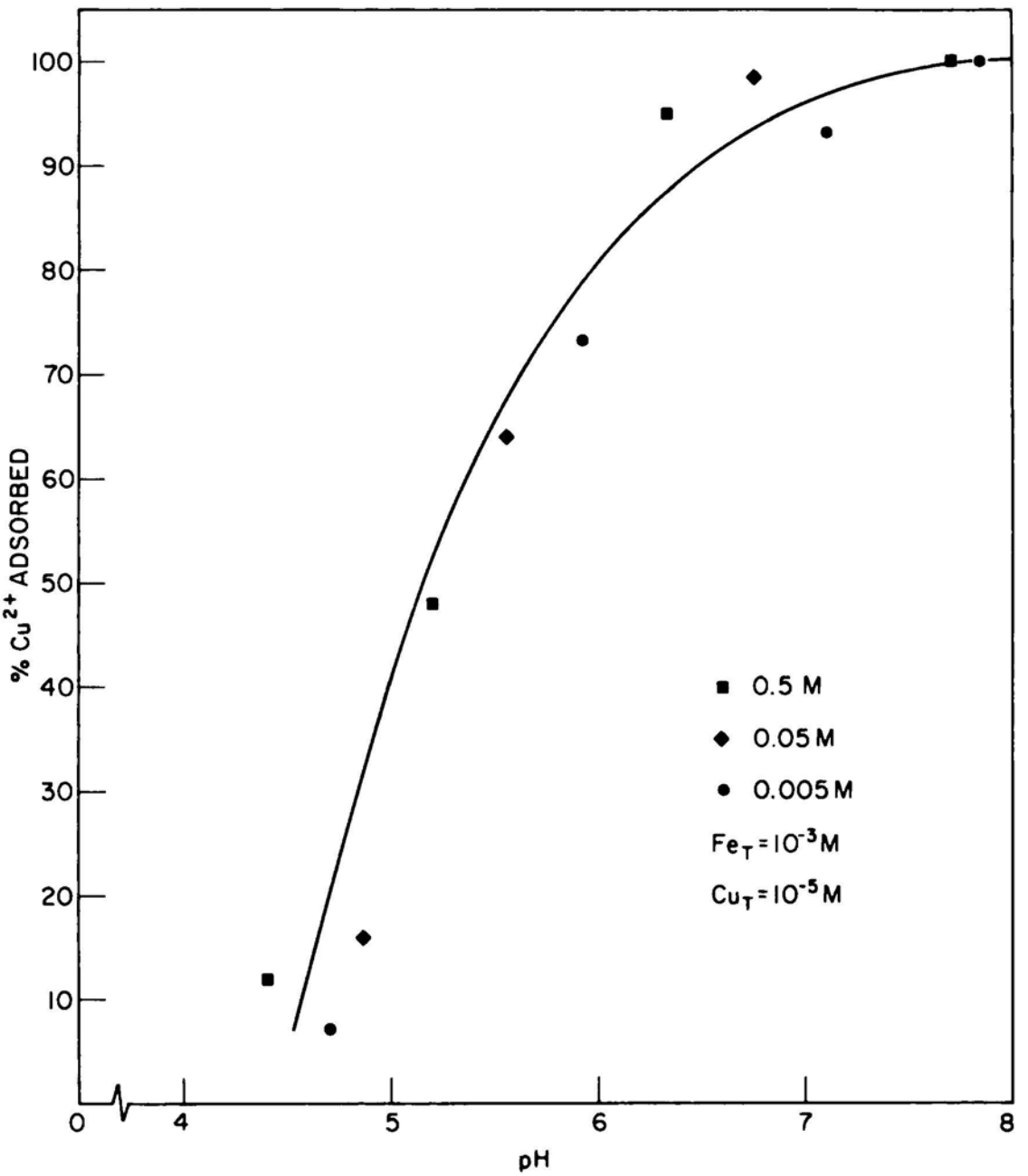

Figure 7. Effect of ionic strength on the Cu^{2+} isotherm for 1×10^{-5}M Cu^{2+} on 1×10^{-3}M hydrous ferric oxide prepared in the different background electrolytes.

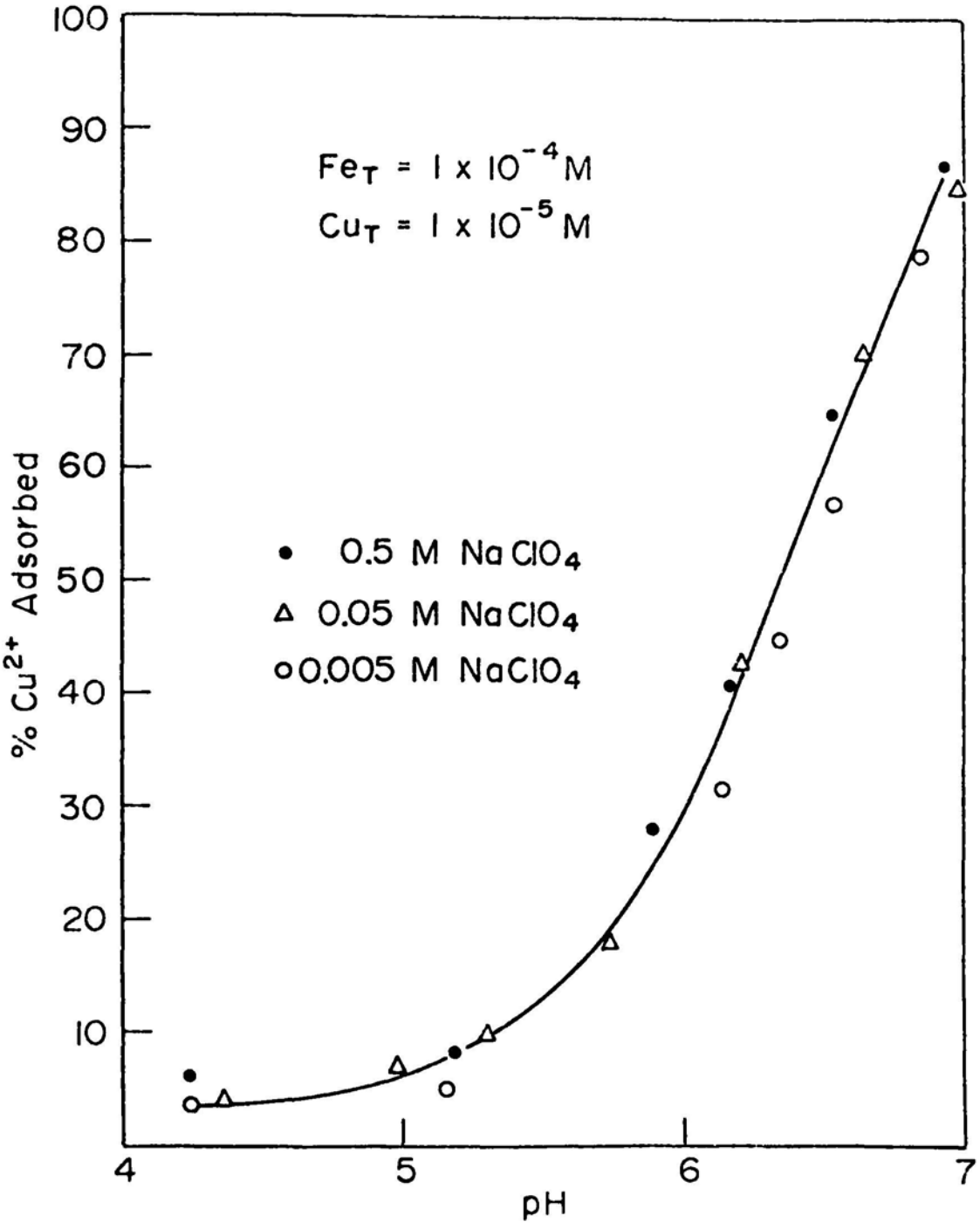

Figure 8. Effect of the ionic strength on the Cu^{2+} isotherm for 1×10^{-5}M Cu^{2+} on 1×10^{-4} hydrous ferric oxide prepared in one large batch and diluted with the appropriate background electrolyte.

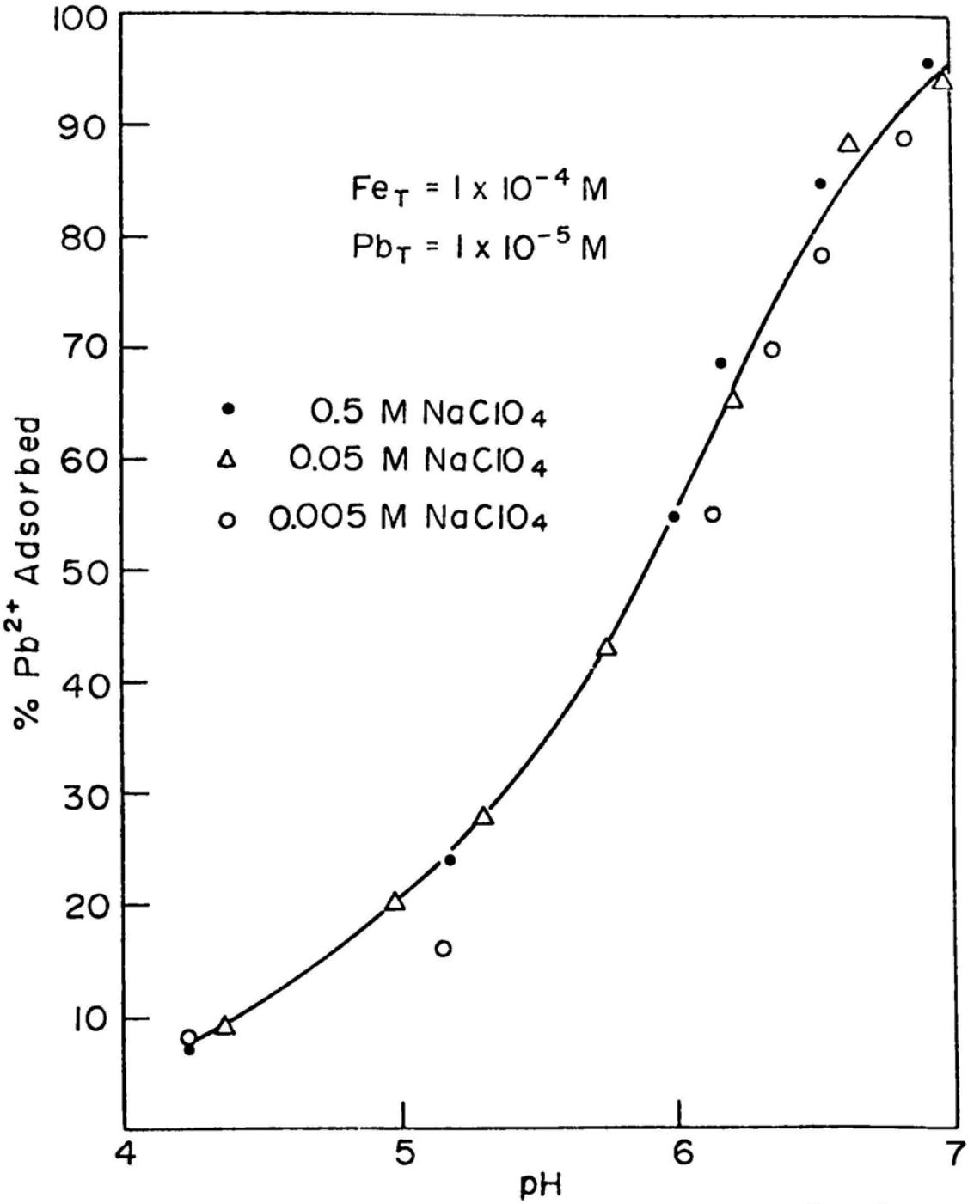

Figure 9. Effect of ionic strength on the Pb^{2+} isotherm for 1 x 10^{-5}M Pb^{2+} on 1 x 10^{-4}M hydrous ferric oxide prepared in one large batch and diluted with the appropriate background electrolyte.

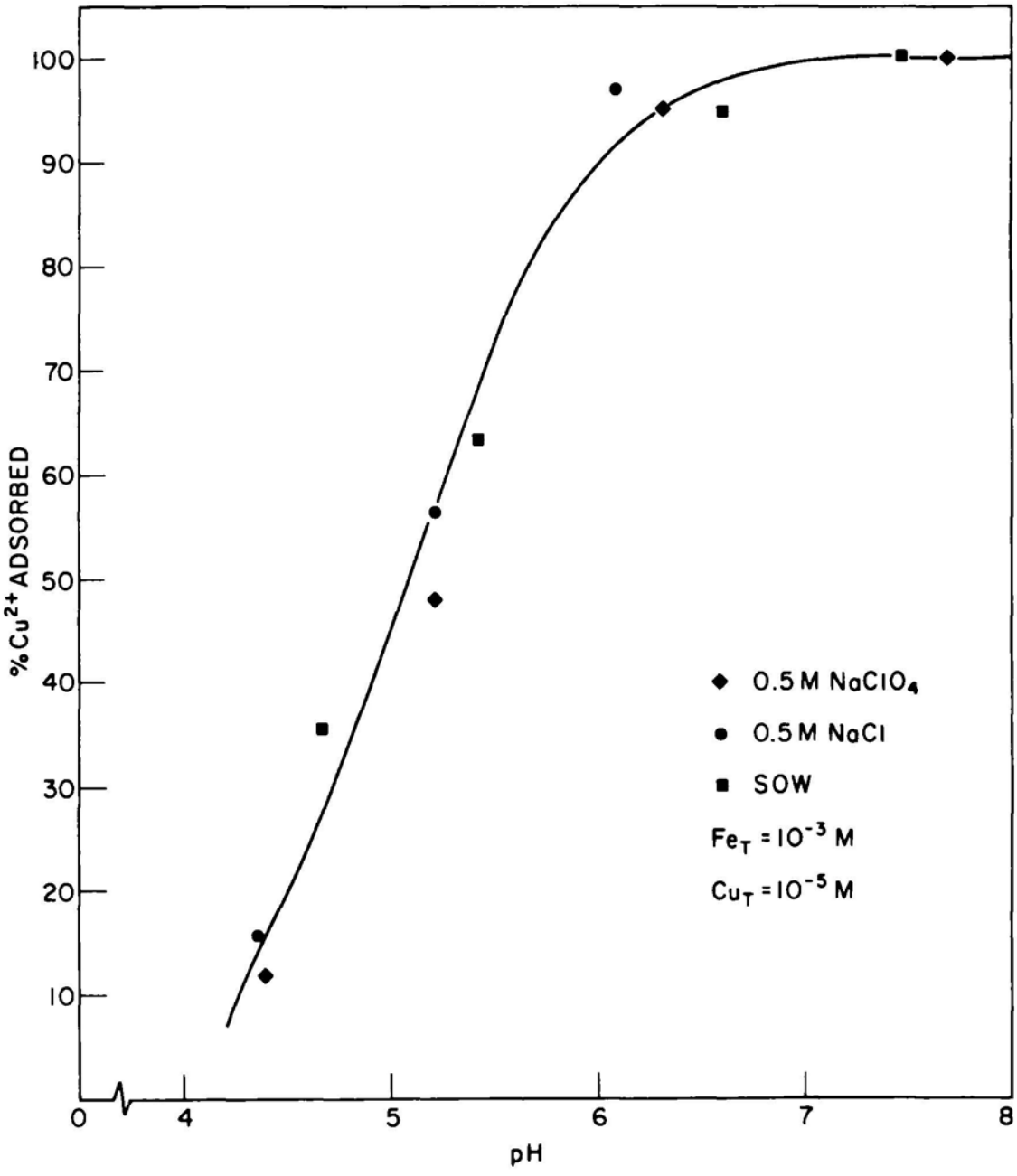

Figure 10. Effect of the background electrolyte composition on the Cu^{2+} isotherm for 1 x 10^{-5}M Cu^{2+} on 1 x 10^{-3}M hydrous ferric oxide prepared in the different background electrolytes.

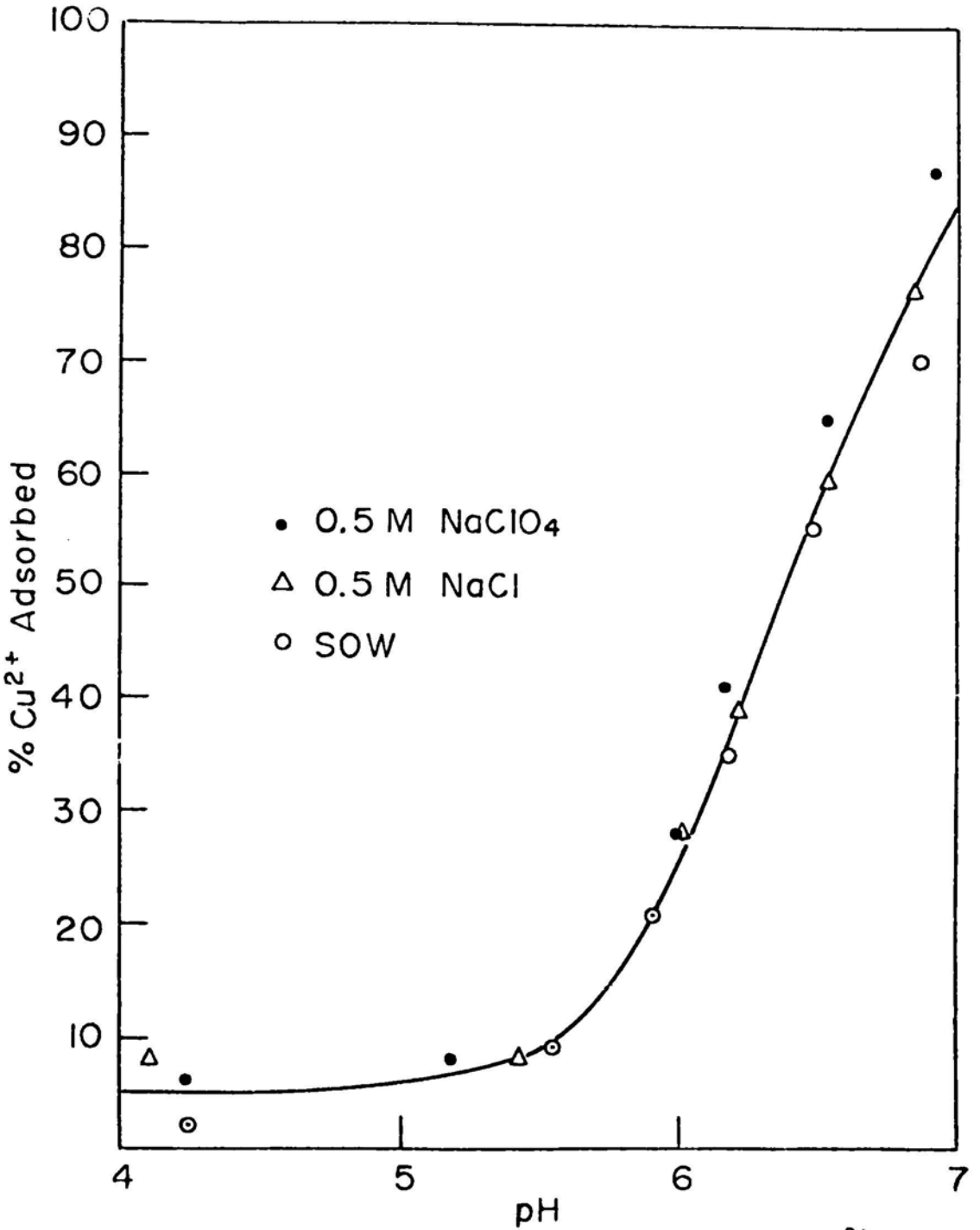

Figure 11. Effect of background electrolyte composition on the Cu^{2+} isotherm for 1 x 10^{-5}M Cu^{2+} on 1 x 10^{-4}M hydrous ferric oxide prepared in one large batch and diluted with the appropriate background electrolyte.

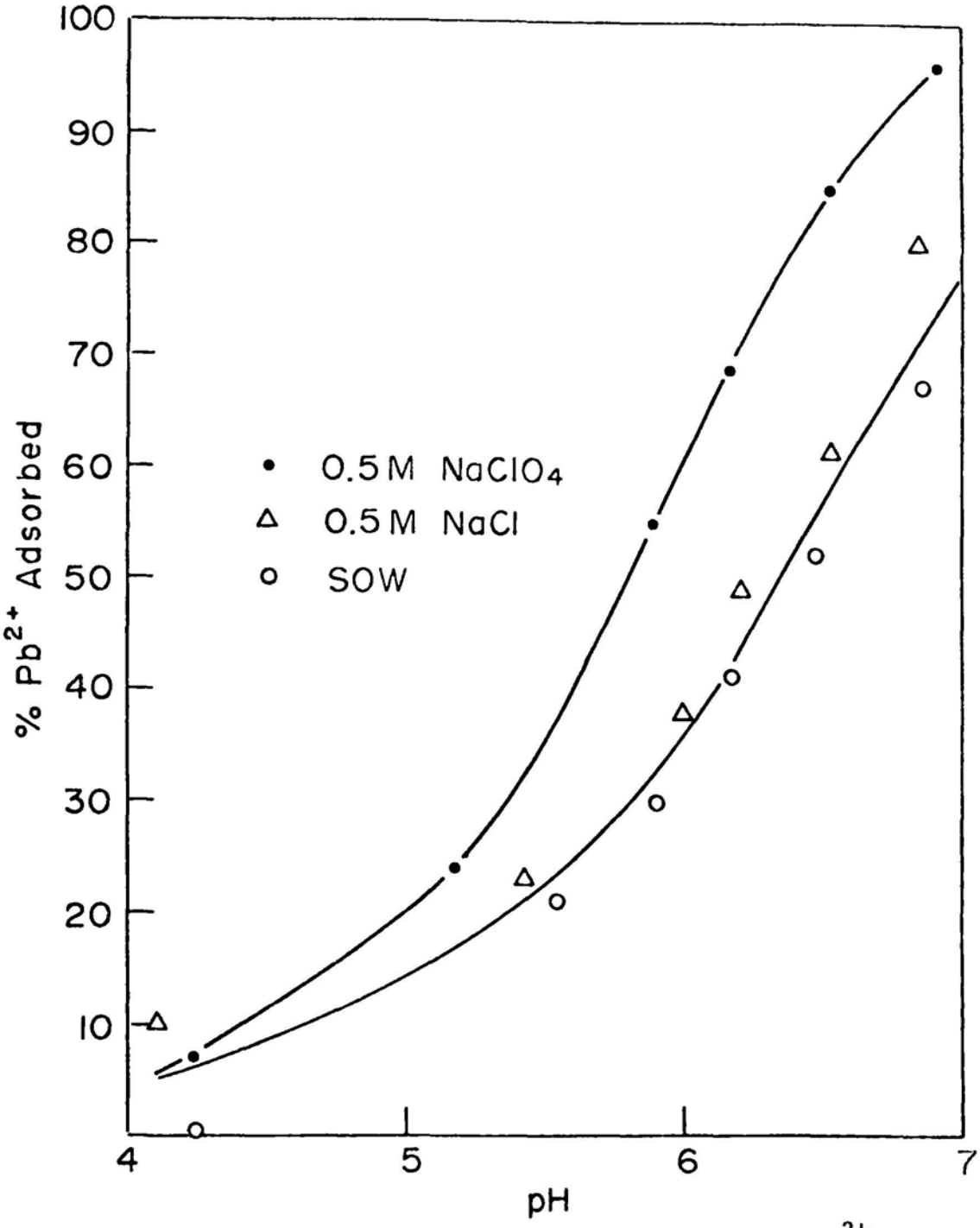

Figure 12. Effect of background electrolyte composition on the Pb^{2+} isotherm for 1×10^{-5} M Pb^{2+} on 1×10^{-4} M hydrous ferric oxide prepared in one large batch and diluted with the appropriate background electrolyte.

batch to batch variability under controlled laboratory conditions. Figure 13 which consolidates the Cu^{2+} data from seven different batches of iron under various conditions of ionic strength and background electrolyte composition, gives a measure of this variability. Some of the low data at high pH may reflect contamination of the filtrate from new apparatus and not true batch to batch variations. Nevertheless there are significant differences among the isotherms obtained with different batches which must be considered when comparing the data of different researchers or applying the results to natural systems.

To elucidate the nature of the reaction, metal and oxide concentrations were systematically varied. The precipitation of the Cu^{2+} and Pb^{2+} hydroxides limited the metal concentrations that could be used to ca. 1×10^{-4}M Cu^{2+} and 4×10^{-4}M Pb^{2+}. The minimum oxide concentration yielding measurable uptake of metals was 5×10^{-5}M.

In the first set of experiments, the hydrous ferric oxide concentration was kept at 1.0×10^{-4}M while the Cu^{2+} concentration was varied. From consideration of a simple mass balance

$$\equiv M\text{-}O^- + Me^{2+} \rightleftarrows \equiv M\text{-}O\text{-}Me^+ \quad ; \quad K = \frac{\{\equiv M\text{-}O\text{-}Me^+\}}{\{\equiv M\text{-}O^-\}[Me^{2+}]} \qquad (1)$$

it was expected that below saturation at a given pH the ratio of adsorbed to free metal would remain constant while the total moles of metal adsorbed increased as long as the available reaction sites were in large excess. As saturation was approached, the ratio of adsorbed to free metal would begin to decrease as the available reaction sites decreased. According to this interpretation, the results shown in Figures 14 and 15 imply that saturation is not approached up to a Cu^{2+}/Fe ratio of 0.2. The ratio $Cu^{2+}_{adsorbed}/Cu^{2+}_{free}$ remained constant while the moles of Cu^{2+} adsorbed increased with increasing Cu^{2+}. Increasing the Cu^{2+} concentration above 1.0×10^{-4}M would have led to precipitation of $Cu(OH)_2$ in the range in which the isotherms showed significant adsorption of Cu^{2+}. The ferric oxide concentration was therefore decreased to 5.0×10^{-5}M and the experiment repeated with the same Cu^{2+} concentrations. It appears that even under these conditions, an approach to saturation cannot be reached before the Cu^{2+} precipitates as $Cu(OH)_2$ (Figures 16-17). The distinction between adsorption and precipitation of Cu^{2+} in these experiments was very clear. Before the onset of precipitation, a gradual decrease in free Cu^{2+} accompanied a gradual increase in pH as base was added. When precipitation of $Cu(OH)_2$ began, a rapid decrease in free Cu^{2+} occurred while the pH remained constant with the addition of base. As previously mentioned, further reduction of the hydrous ferric oxide concentration to 1.0×10^{-5}M resulted in negligible Cu^{2+} adsorption in the pH range 4-7.

Since the Cu^{2+} hydrolysis and precipitation made it impossible to demonstrate saturation of the hydrous ferric oxide with Cu^{2+}, the experiments were repeated with Pb^{2+} which precipitates as $Pb(OH)_2$ at a slightly higher pH than Cu^{2+} precipitates as $Cu(OH)_2$, but gives a similar isotherm on hydrous ferric oxide. The results shown in Figures 18 and 19 are not as straightforward as those for Cu^{2+}. During the generation of the isotherms, the

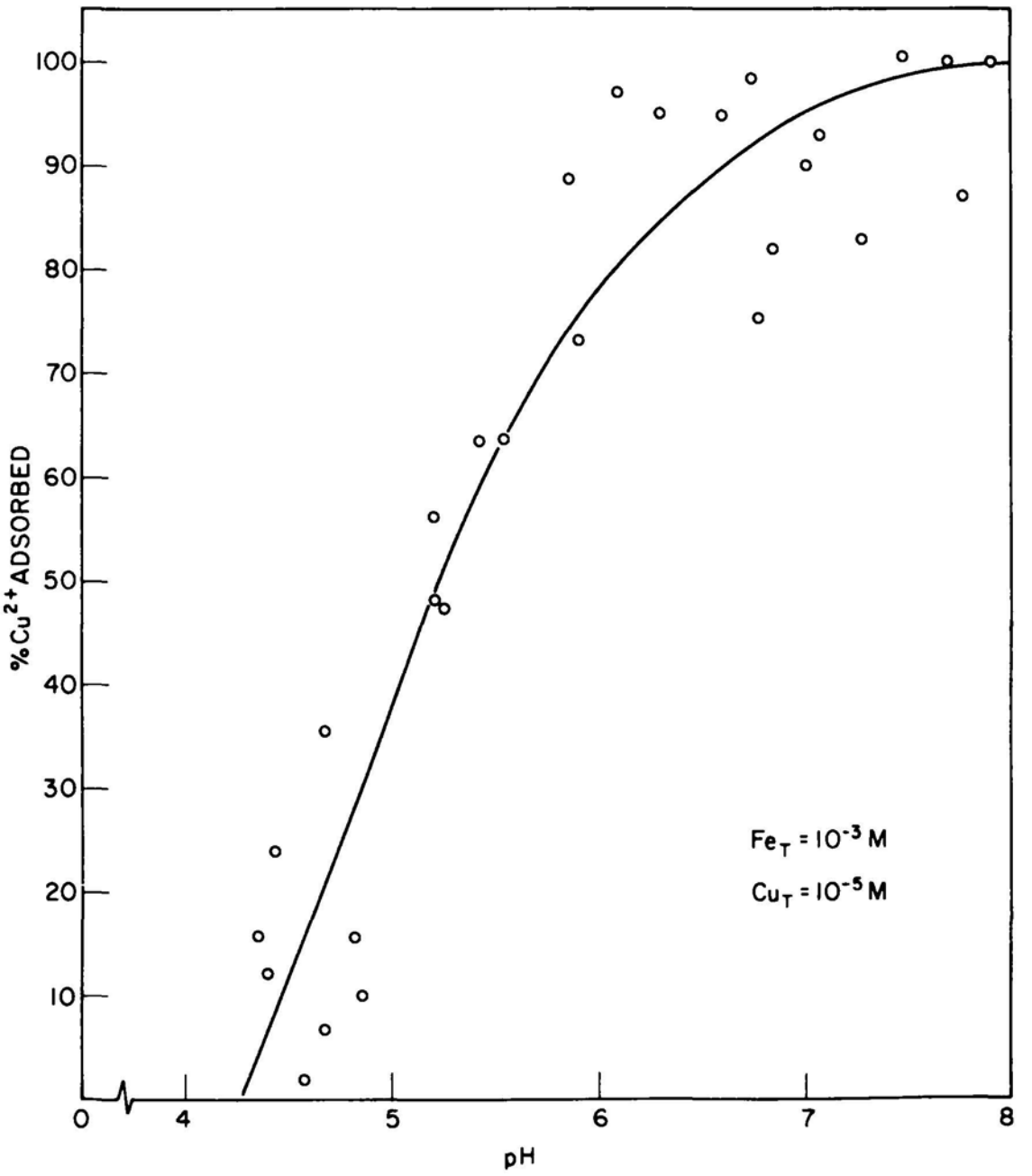

Figure 13. Isotherms for 1 x 10^{-5}M Cu^{2+} on 1 x 10^{-3}M hydrous ferric oxide under various conditions of ionic strength and background electrolyte composition obtained with different batches of hydrous ferric oxide prepared in the different background electrolyte.

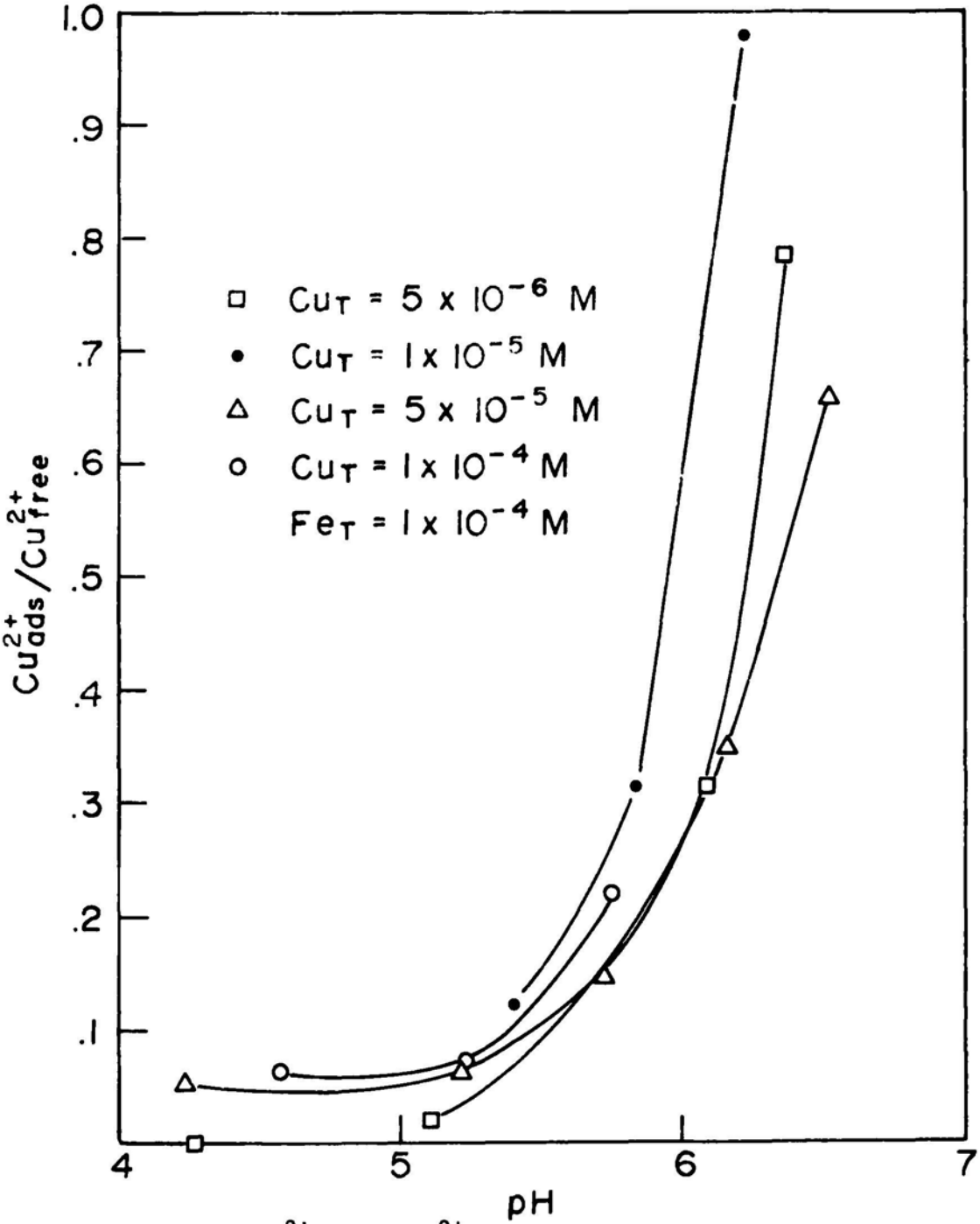

Figure 14. The ratio $Cu^{2+}_{adsorbed}/Cu^{2+}_{free}$ as a function of pH for variable Cu_T on 1 x 10^{-4}M hydrous ferric oxide.

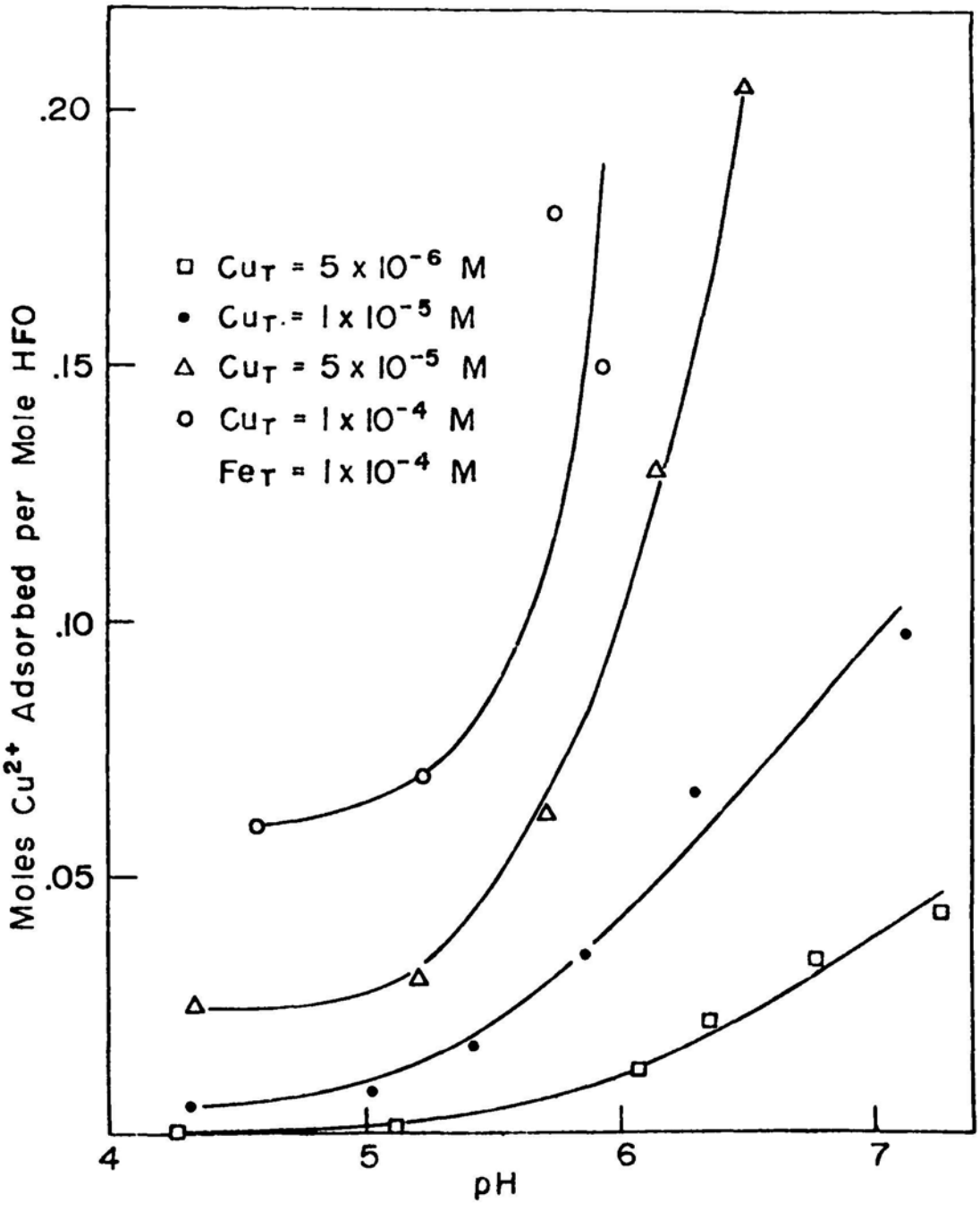

Figure 15. Moles of Cu^{2+} adsorbed per mole hydrous ferric oxide as a function of pH for variable Cu_T on 1 x 10^{-4}M hydrous ferric oxide.

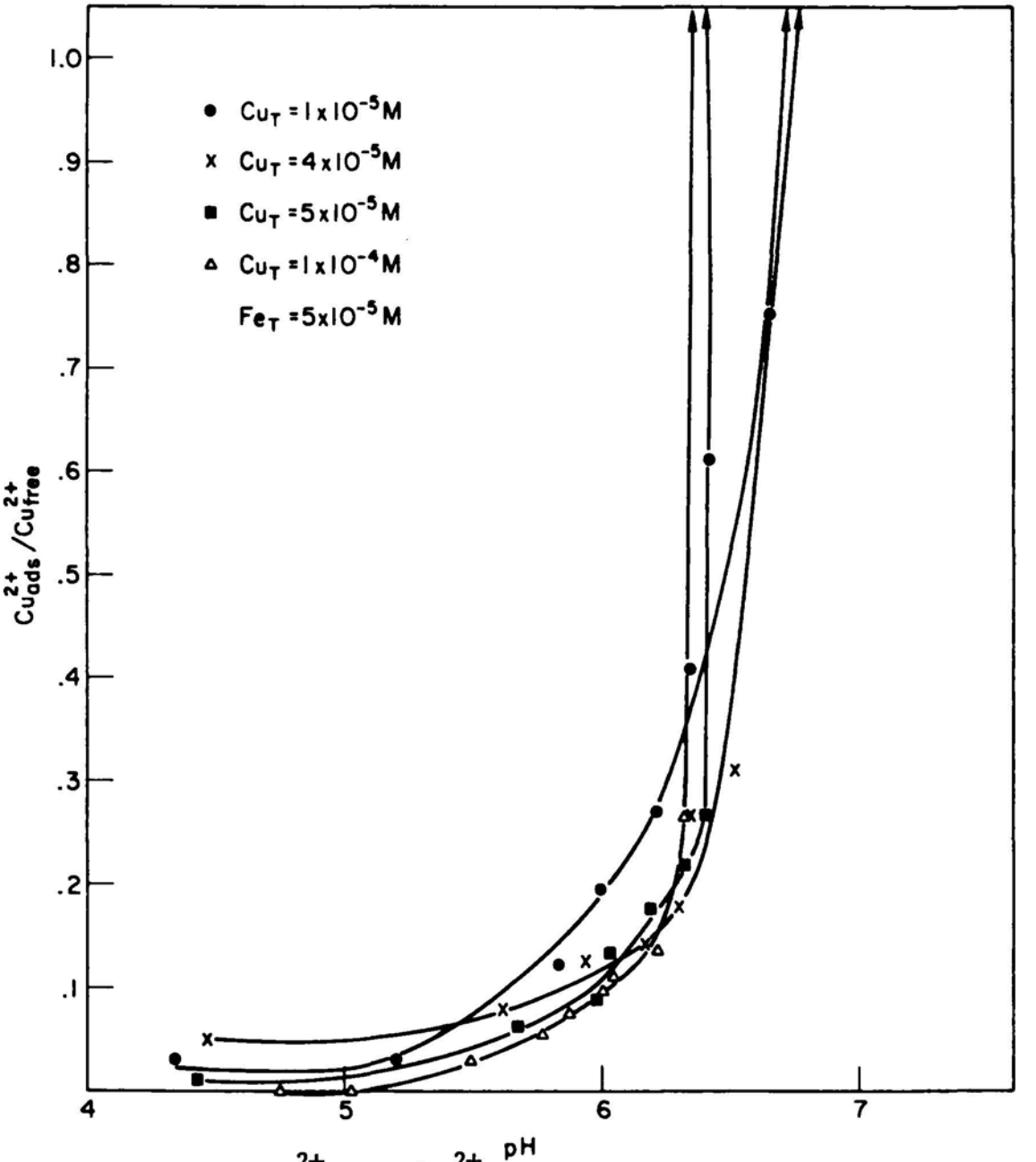

Figure 16. The ratio $Cu^{2+}_{adsorbed}/Cu^{2+}_{free}$ as a function of pH for variable Cu_T on 5.0×10^{-5}M hydrous ferric oxide.

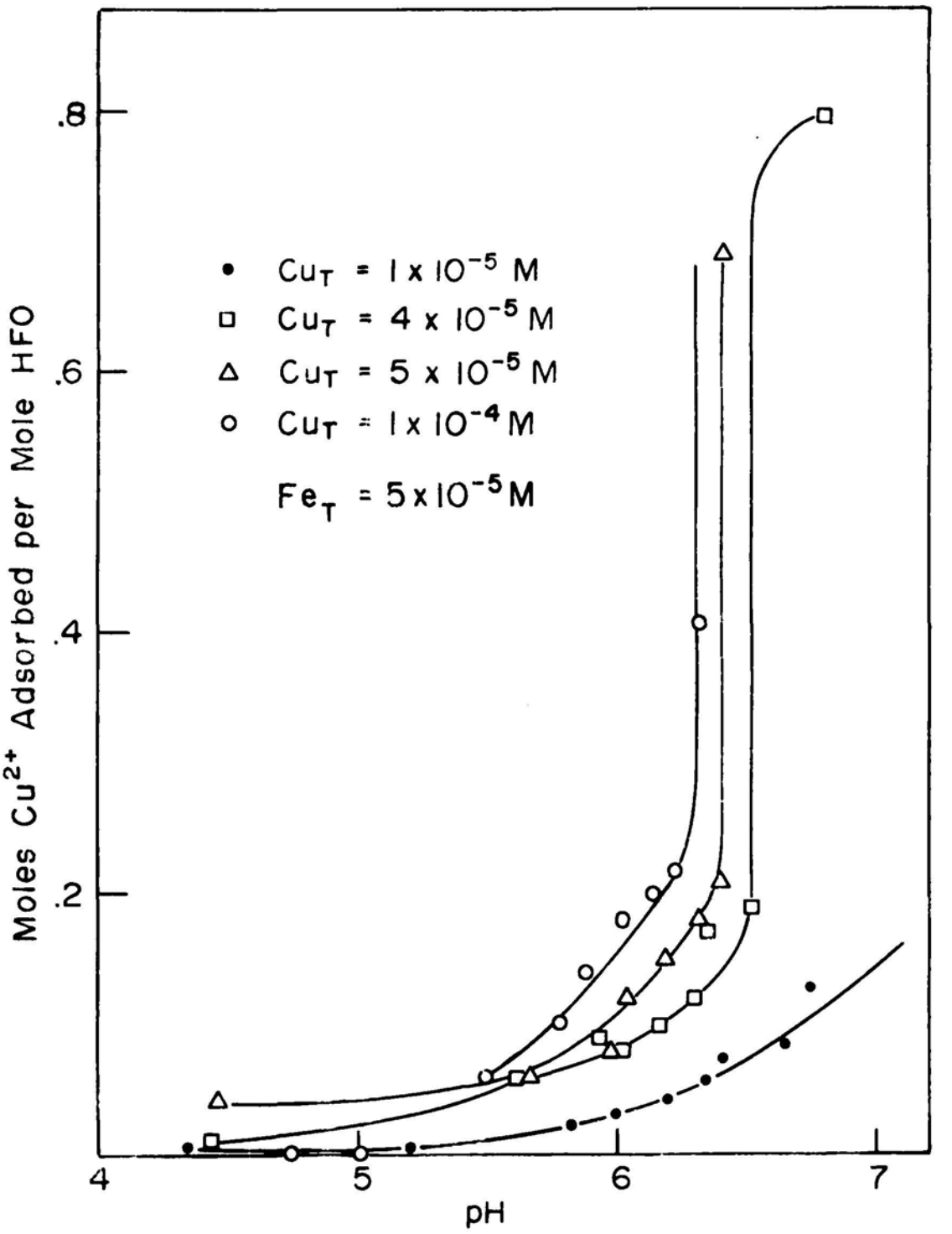

Figure 17. Moles of Cu^{2+} adsorbed per mole hydrous ferric oxide as a function of pH for variable Cu_T on 5.0×10^{-5} M hydrous ferric oxide.

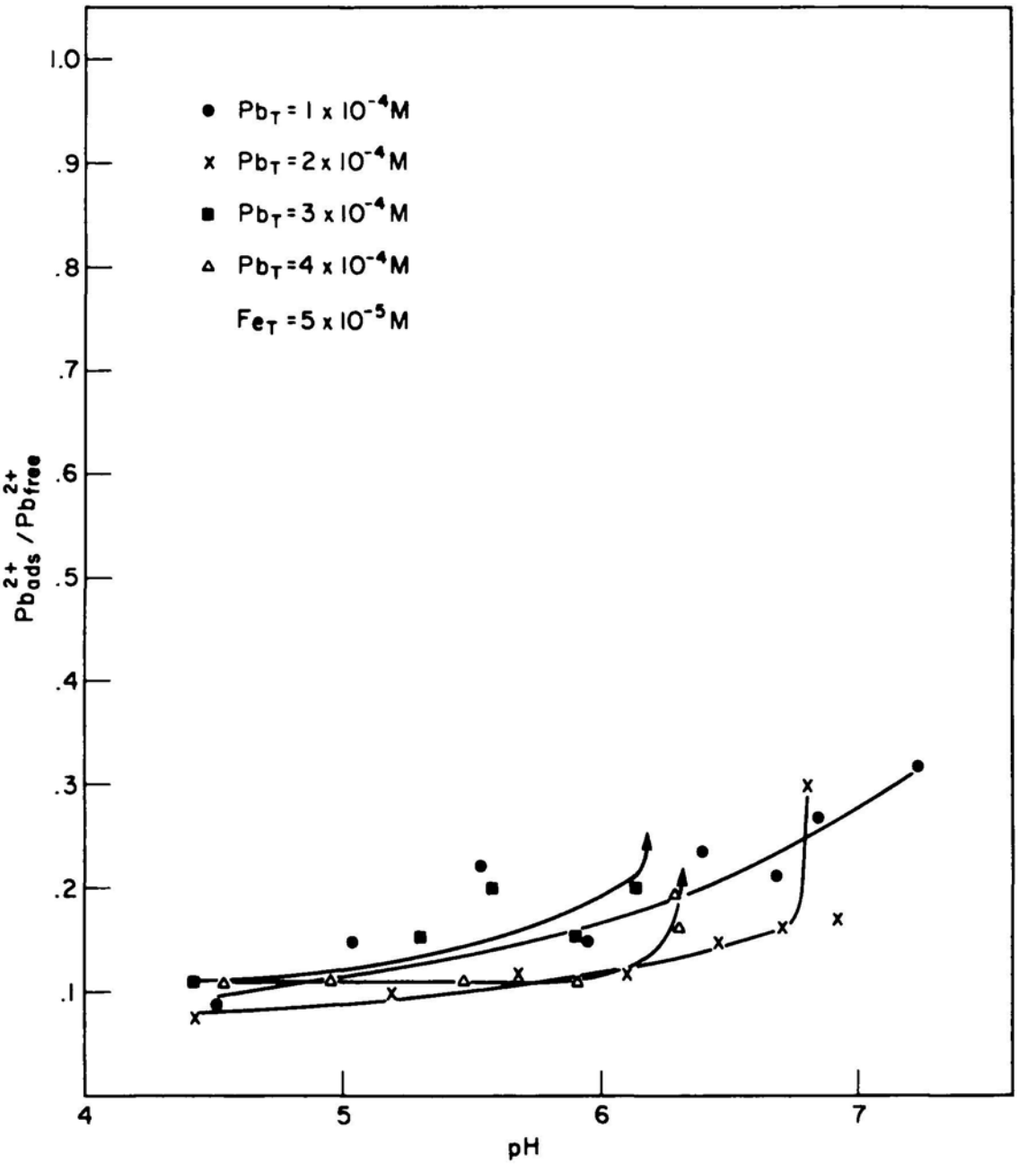

Figure 18. The ratio of $Pb^{2+}_{adsorbed}/Pb^{2+}_{free}$ as a function of pH for variable Pb_T on 5.0×10^{-5}M hydrous ferric oxide.

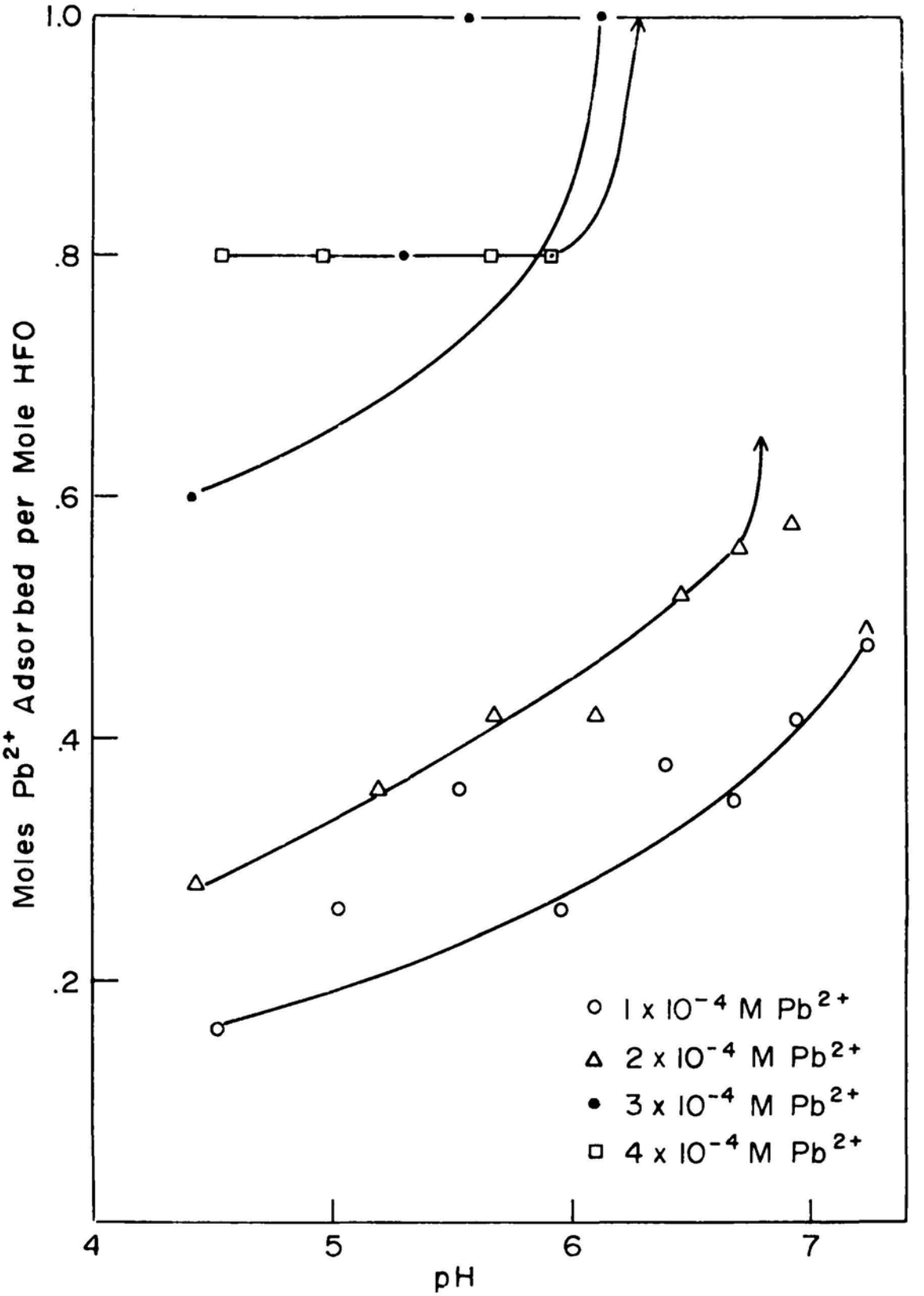

Figure 19. Moles of Pb^{2+} adsorbed per mole hydrous ferric oxide as a function of pH for variable Pb_T on 5.0 x 10^{-5} M hydrous ferric oxide.

Pb^{2+} solutions apparently became supersaturated with respect to $Pb(OH)_2$ and an addition of base actually lowered the pH if precipitation commenced. The complex and variable hydrolysis of Pb^{2+} in these solutions reflects the known polynuclear behavior of Pb^{2+} hydrolysis products. Britton (37) in a study of the precipitation of trace metal hydroxides, found that K_{sp} for $Pb(OH)_2$ increased with the amount of alkali added, ranging from 3×10^{-19} to 1.35×10^{-15}. A phenomenon of this kind is indicated in the data presented here. At high Pb^{2+} concentration (4.0×10^{-4}M) the precipitation of $Pb(OH)_2$ caused the hydrous ferric oxide to coagulate and a white solid was carried down with the brick red ferric oxide. Before the appearance of the white solid, however, the distinction between adsorption and precipitation of the hydroxide was not as clear for Pb^{2+} as it was for Cu^{2+}. Despite these difficulties, an approach to saturation is suggested with the highest Pb^{2+} concentration at a 0.8Pb/Fe ratio.

The expected increase in Cu^{2+} and Pb^{2+} adsorption with increasing Fe_T at a given pH, is shown in Figures 20 and 21. The reduction of the data to

$$\frac{Cu^{2+}_{adsorbed}}{Cu^{2+}_{free} Fe_T} \qquad (1)$$

and

$$\frac{Pb^{2+}_{adsorbed}}{Pb^{2+}_{free} Fe_T} \qquad (2)$$

presented in Figures 22 and 23, respectively shows that the increase is approximately proportional to the concentration of the oxide. The high points in the Cu^{2+} plot at low pH and the low points in the Pb^{2+} plot at high pH reflect large indeterminant errors in the isotherms.

COMPETITION BETWEEN METALS FOR THE HYDROUS FERRIC OXIDE

It was impossible to demonstrate competition between Pb^{2+} and Cu^{2+} for the iron. This was consistent with the difficulties encountered in demonstrating saturation for either of the metals. An apparent competition was demonstrated between Cu^{2+} and Fe^{2+} when 1.0×10^{-5}M Cu^{2+} and 5.0×10^{-4}M Fe^{2+} were present with 4.0×10^{-4}M hydrous ferric oxide in an O_2-free system.* This result is shown in Figure 24 as a large depression in the isotherm compared to the same system in the absence of Fe(II). This demonstration is of academic interest only, as an O_2-free system is not applicable to seawater but it does indicate the possibility of competition if combined trace metal concentrations are sufficiently high.

* The N_2 used to exclude CO_2 from the system was also passed through a trap containing Cu metal in NH_4OH solution to remove O_2, a second trap containing HCl to remove NH_3 and a water trap to remove NH_4Cl and HCl.

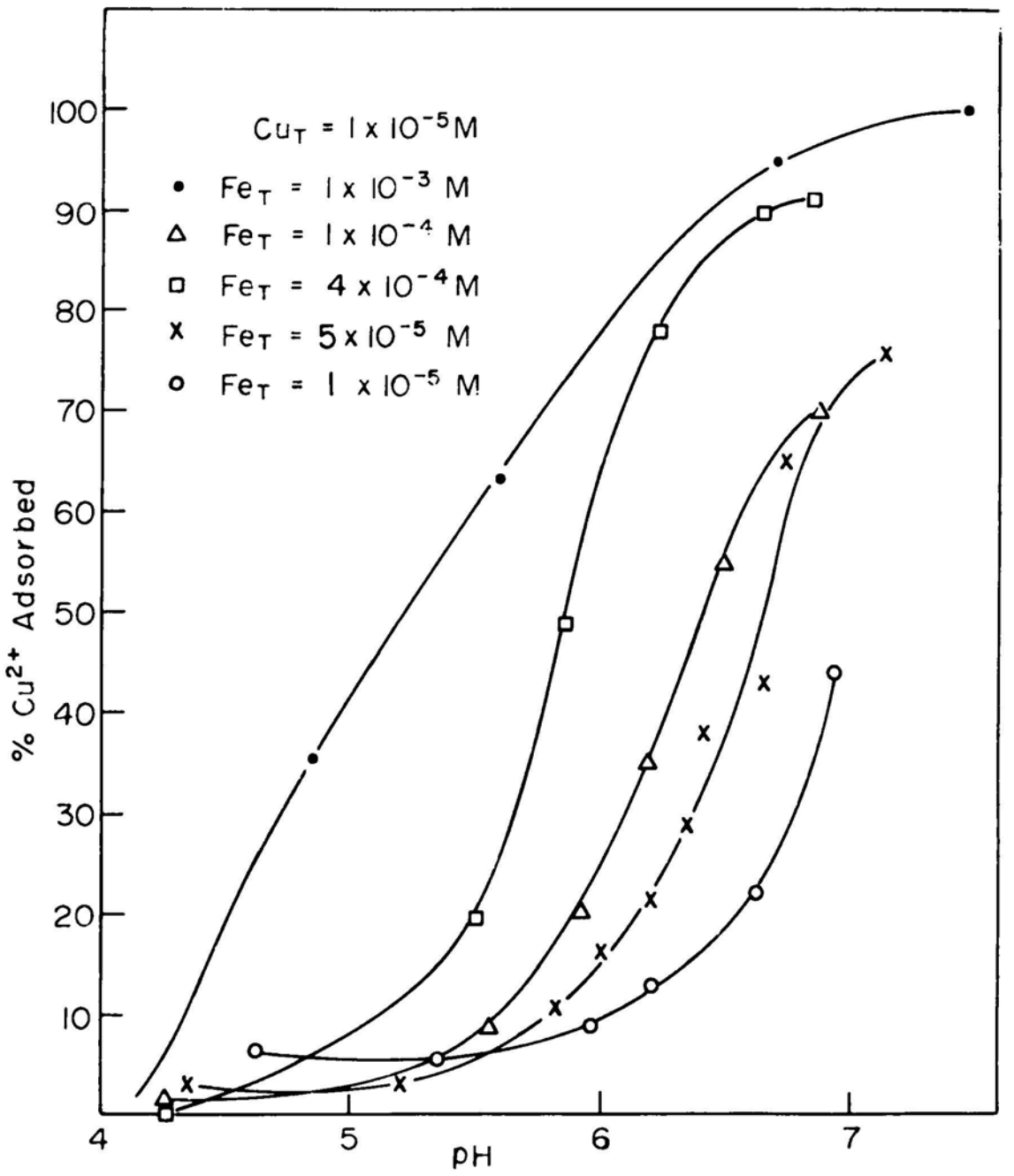

Figure 20. Per cent Cu^{2+} adsorbed as a function of pH for various concentrations of hydrous ferric oxide in S.O.W.

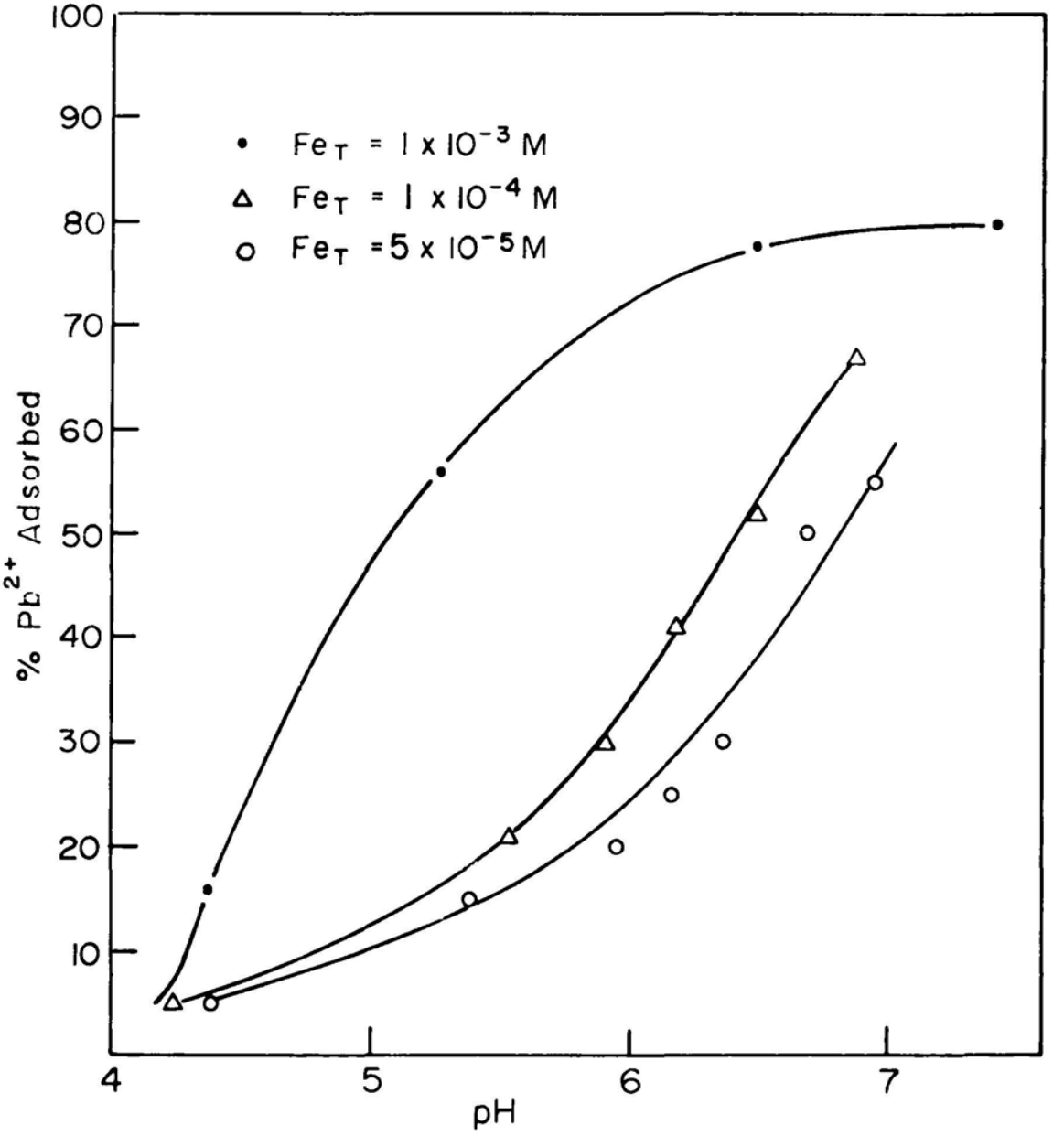

Figure 21. Per cent Pb^{2+} adsorbed as a function of pH for various concentrations of hydrous ferric oxide in S.O.W.

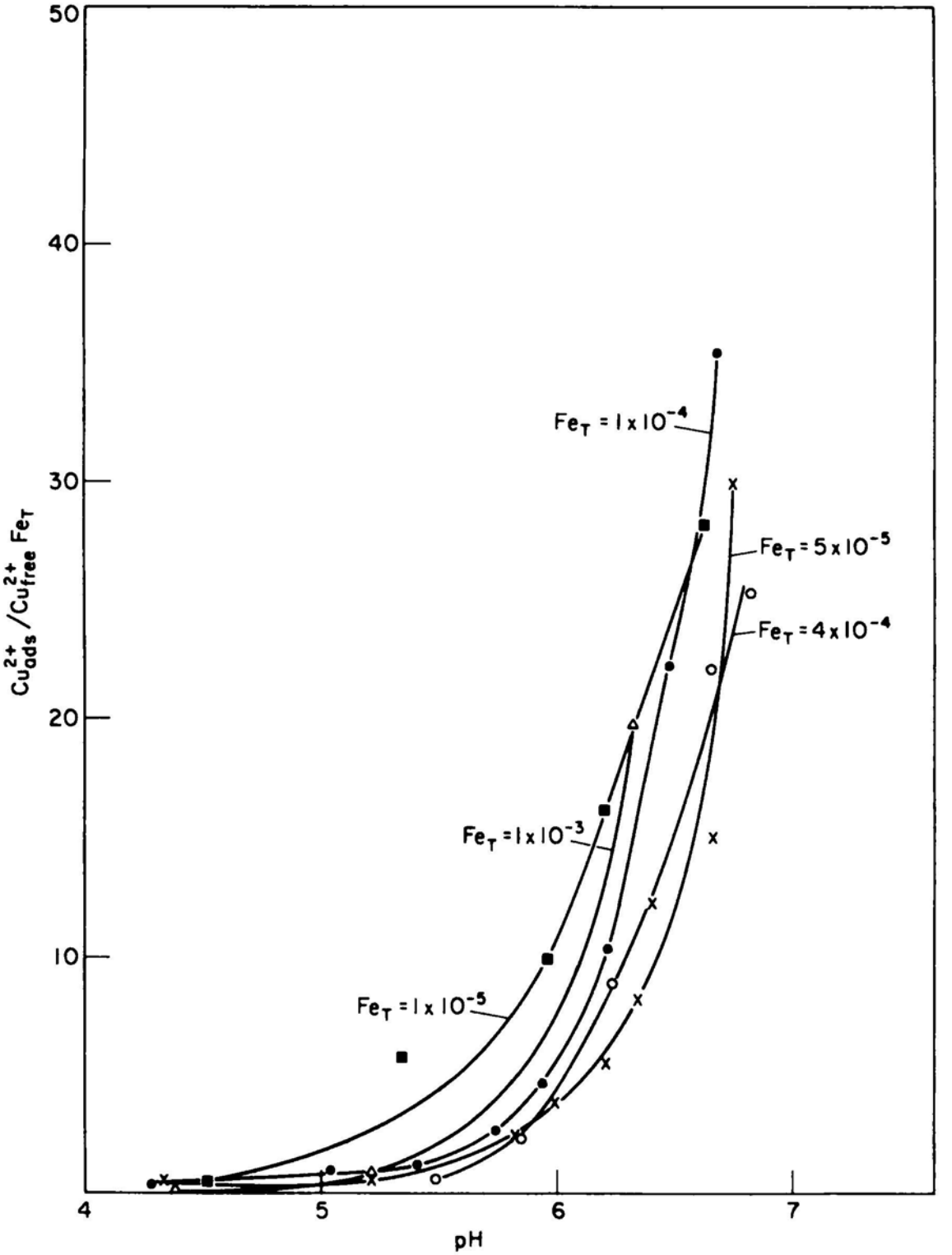

Figure 22. Reduction of data from isotherms for 1.0×10^{-5} M Cu^{2+} on various concentrations of hydrous ferric oxide in S.O.W. to $Cu^{2+}_{adsorbed}/Cu^{2+}_{free}Fe_T$ as a function of pH.

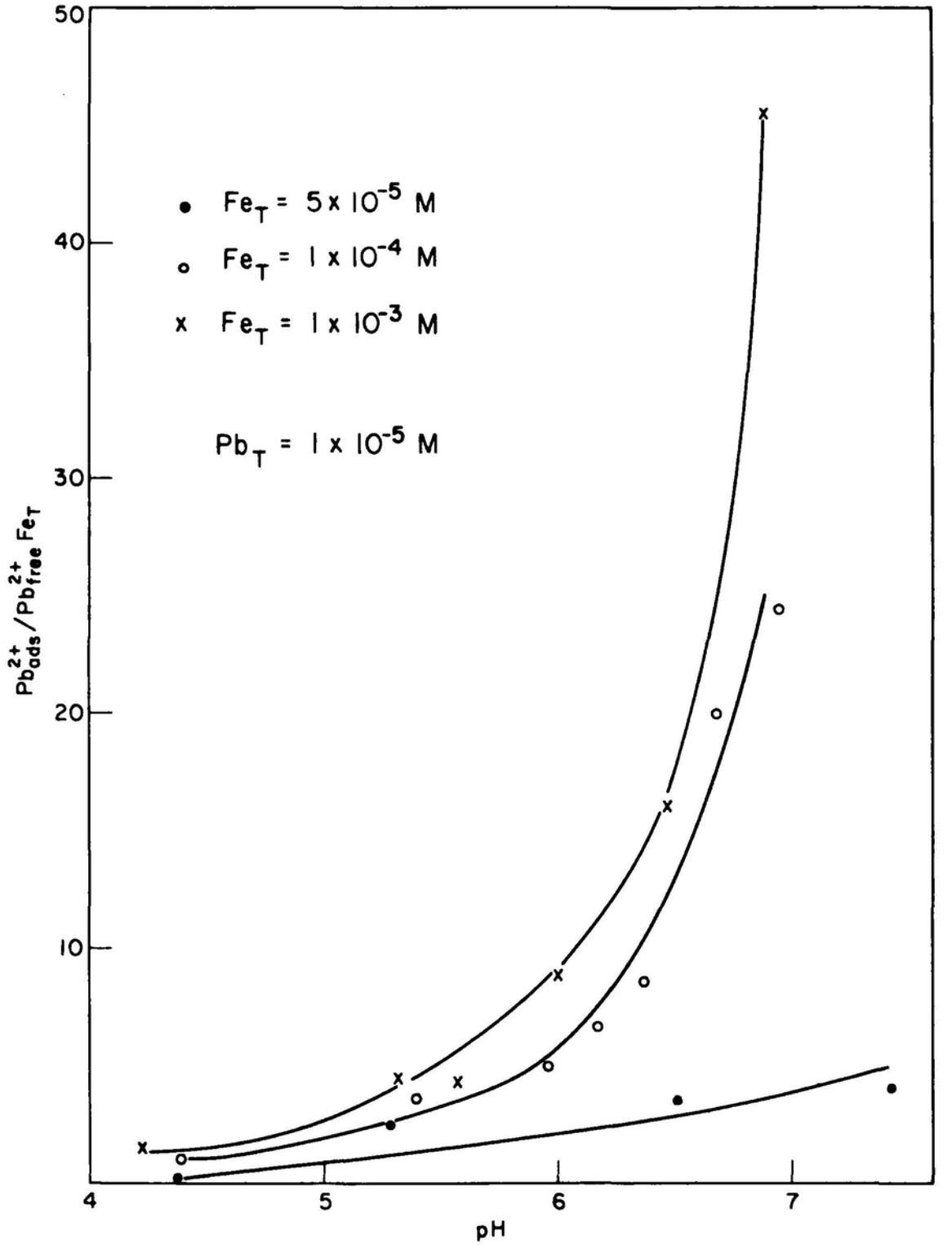

Figure 23. Reduction of data from isotherms for 1.0×10^{-5} M Pb^{2+} on various concentrations of hydrous ferric oxide in S.O.W. to $Pb^{2+}_{adsorbed}/Pb^{2+}_{free}Fe_T$ as a function of pH.

SECTION 4

DISCUSSION

The mechanism by which hydrous metal oxides remove trace metals from solution has been postulated by various workers to be adsorption, chemisorption, ion exchange, surface complexation and coprecipitation. Several simple, well-defined experimental systems yielded data which could be fitted to equations derived for models based on these mechanisms.

The electrical double layer theory and numerous modifications treat the phenomenon of electrostatic adsorption of ions on a charged surface. James and Healy added a term to the established double layer treatment to explain the relationship between hydrolysis of metal ions and their specific adsorption (chemisorption). The surface complexation model proposes a chemical reaction between surface sites and metal ions in solution for which the equilibrium constants are modified by the surface charge. All of the mathematical models require that the data can be reduced to an apparent constant for a given pH and a given background electrolyte according to a mass law expression

$$K = \frac{\{\equiv M\text{-}O\text{-}Me^{+}\}}{\{\equiv M\text{-}O^{-}\}[Me^{2+}]} \qquad (1)$$

As the reduction in Figs. 14, 16, 18, 22 and 23 demonstrates, the reaction of Cu^{2+} and Pb^{2+} with amorphous ferric oxide is, to a first approximation proportional to the free metal concentration in solution and to the amount of oxide over the range 5×10^{-6}M to 4×10^{-4}M metal and 5×10^{-5}M to 1×10^{-3}M oxide.

To reduce the data further to test equation 1, requires an estimate of the total number of reactive sites on the oxide in order to calculate $\{\equiv M\text{-}O^{-}\}$. The acid-base titration data are of little help for this purpose as not all of the acid-base sites appear to be titrated in the pH range of interest. An estimate of total reactive sites based on such data would result in orders of magnitude underestimation of the removal of Cu^{2+} and Pb^{2+} by the iron. Upper and lower limits for the number of reactive sites can be obtained directly from the adsorption data. The Pb^{2+} data (Figure 19) provides the lower limit of 0.8 site/Fe; while an upper limit of 1.5 site/Fe is implied from the Fe(II)-Cu competition experiment (Figure 24). This is consistent with the estimate obtained by Davis (36) of 0.87 site/Fe on the basis of Yates (38) data obtained from rapid tritium exchange experiments. Figure 25 shows the reduction of the data using a value of 1 site/Fe for the Cu^{2+} isotherms in seawater for all values of Cu_T and Fe_T. It should be noted

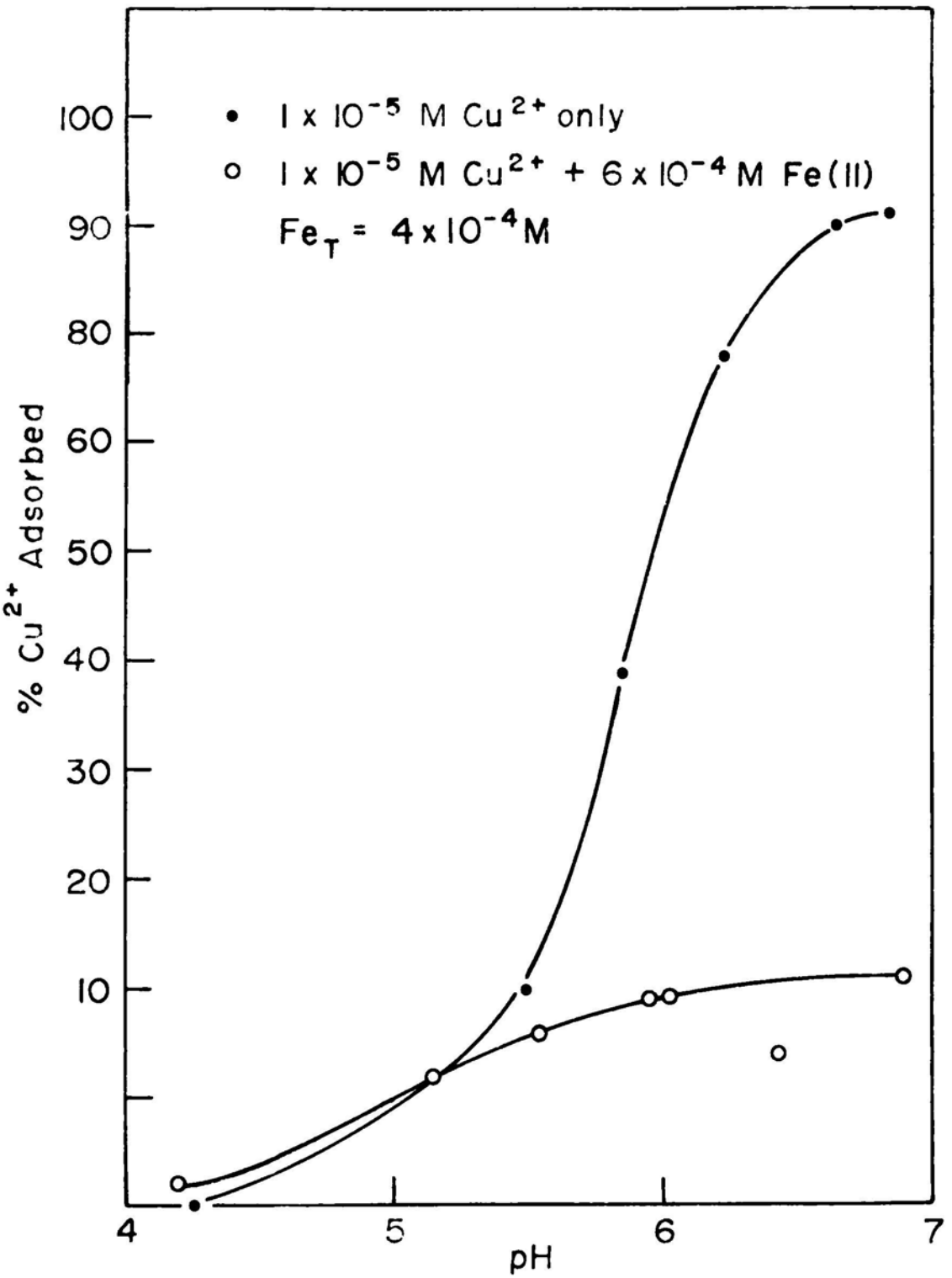

Figure 24. Depression of the isotherm for 1.0×10^{-5}M Cu^{2+} on 4.0×10^{-4}M hydrous ferric oxide in S.O.W. in the presence of 6.0×10^{-4}M Fe^{2+}.

both that the data are consistent with the mass law expression and that since all the isotherms were below saturation, this is not a sensitive test of the value chosen for total reactive sites. Although the Pb^{2+} data would provide a more sensitive test, their scatter renders such reduction meaningless. The curve in Figure 25 provides a convenient means to predict Cu^{2+} removal by the iron oxide for any combination of concentrations and pH.

The very complex system of amorphous ferric oxide in seawater behaves in a remarkably simple way with respect to Cu^{2+} and Pb^{2+} removal. There is no effect of ionic strength, no effect of background electrolyte (except for the expected Cl^- effect on Pb^{2+}), no effect of aging, no difference whether the iron is precipitated in the presence or absence of the metal. Such simplicity was not expected on the basis of the various mechanisms that have been proposed.

The expected effect of ionic strength depends to some extent on the model being considered. The ionic strength enters into electrical double layer calculations and affects the coulombic interactions between the charged surface and the adsorbing ions by changing the thickness of the double layer. The parameter 1/K, which can be conceived of as the distance between the plates of a hypothetical electrical condenser representing the electrical double layer is 10.0 nm in 1.0×10^{-3}M NaCl and reduces to 0.36 nm in 0.7M NaCl (39). The collapse of the electrical double layer at high ionic strength decreases the diffuse layer potential. What effect this has on adsorption of trace metal cations, which are specifically adsorbed against the electrostatic repulsion of a positively charged surface, is unclear.

In all cases, however, the coulombic interactions in the adsorption process can only play a role for reactions resulting in a net change of charge. The remarkable consistency of the isotherms for various ionic strengths invites a speculation that the reaction of iron oxide with Cu^{2+} and Pb^{2+} results in no net change in charge in the pH range of interest. For example, two protons may exchange for one metal ion. This is reinforced by the aging study which demonstrates a clear change in charge (evidenced by a change in uptake of acid by the solid) with no concomitant change in the isotherm.

Britton (37) in extensive studies of the precipitation of hydroxides found that in general the amount of base needed to precipitate a metal hydroxide did not correspond to the computed stoichiometric amount. He concluded that other anions were incorporated into the solid forming what he calls "basic salts". Such non-stoichiometric precipitation would lead to the observed batch to batch variations, but it also implies a possible effect of the background electrolyte on the nature of the iron oxide. The effect of the background electrolyte on the formation of the crystalline ferric oxides has been reported (12). Whatever effect the background electrolyte may have on the nature of the amorphous iron oxide, however, it is not reflected in the isotherms for Cu^{2+} and Pb^{2+}.

It is puzzling that the release of 1.3 eq/mole of H^+/Fe over 24 hours of aging is not accompanied by any change in the Cu^{2+} isotherms. There is a strong implication that the protons lost in aging are not the exchangeable protons on the reactive sites. This may be a consequence of different

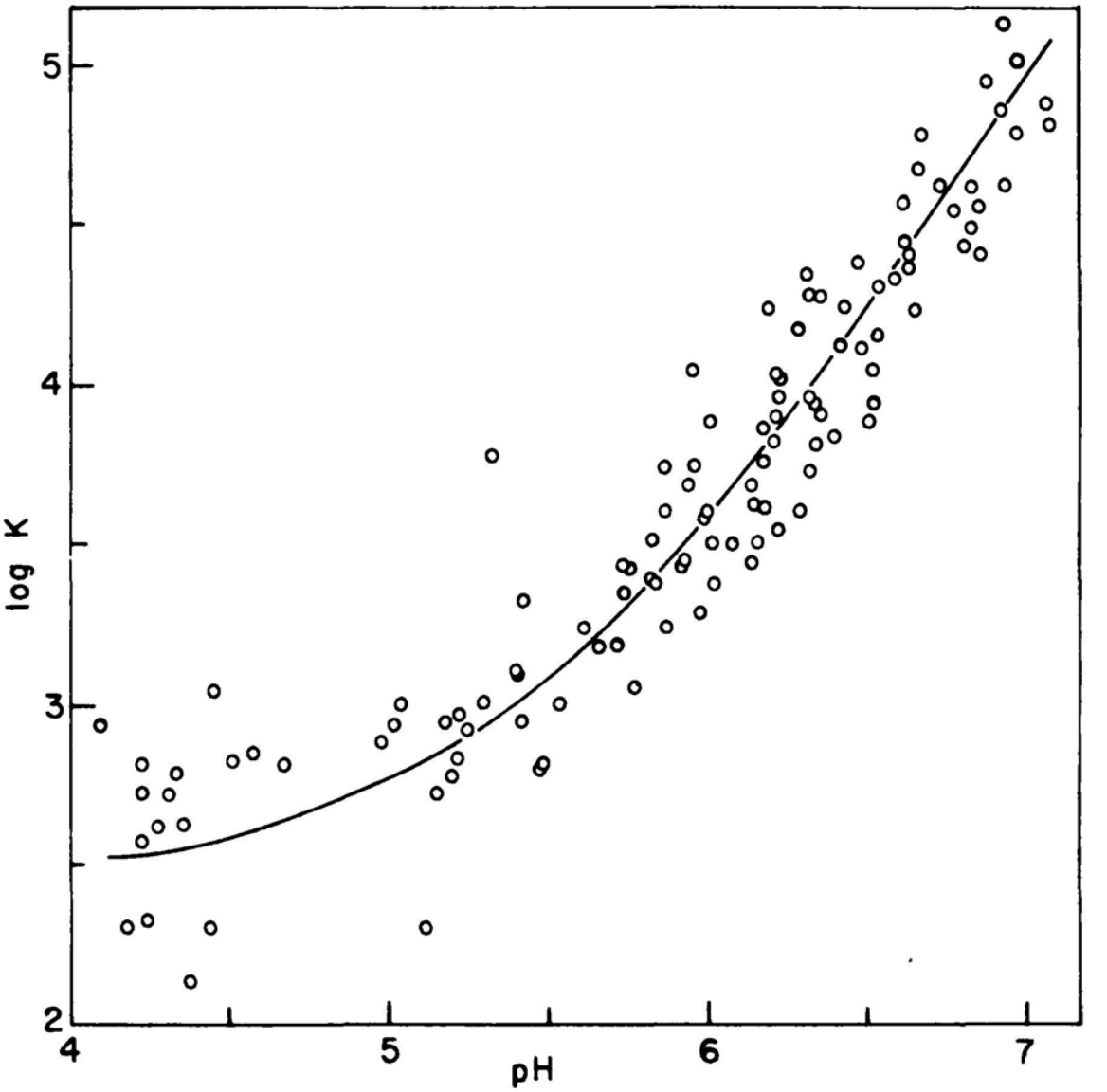

Figure 25. Log K as a function of pH for all Cu^{2+} data where:

$$K = \frac{Cu^{2+}_{adsorbed}}{(Cu_T - Cu^{2+}_{adsorbed})(Fe_T - Cu^{2+}_{adsorbed})}$$

coordination of the oxygen atoms or of geometrical inaccessability of some of the oxygen atoms. Dousma and de Bruyn (6) discuss the polymerization of Fe(III) oxide and note that in addition to the olation processes involving -OH addition to iron oxide polymers, oxolation also occurs. This process is represented by

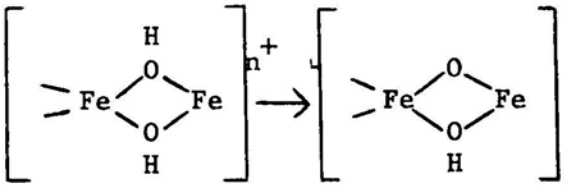

(1)

The oxo bridges thus formed react very slowly with acid. Oxolation would explain the release of acid over the first 24 hours. The oxygen atoms involved in oxolation are already bound to two iron atoms and are not likely to be the reactive sites. That the acid-base sites with rapidly exchangeable protons and the coordination sites for Cu^{2+} are indeed the same is supported by the dependence of the apparent adsorption constant (K) on pH. Note that from pH 6 to 7 the apparent constant increases by an order of magnitude (Figure 15).

The capacity of amorphous hydrous ferric oxide for metal ions makes the meaning of the terms "surface" and "adsorption" somewhat arbitrary. It becomes necessary to provide a more satisfactory image of the system than that of an interface separating two semi-infinite phases. One is clearly not concerned with the interface between the visible precipitate and the bulk solution, but rather the interface between some microstructure and its immediately surrounding water. Amorphous hydrous ferric oxide has been described as "amorphous, randomly crosslinked aggregates containing large and indefinite amounts of water" (40). This description calls to mind the structure of a swollen ion exchange resin which is permeable to hydrated ions. The ions are free to diffuse throughout the structure and are not restricted to external "surface" sites.

The formation of hydrous ferric oxide proceeds from the hydrolysis of the hexahydrated aquo ion

$$Fe(H_2O)_6^{3+} \rightarrow Fe(H_2O)_5OH^{2+} + H^+$$

to formation of the dimer

$$2Fe(H_2O)_5OH^{2+} \rightarrow (Fe(H_2O)_5OH)_2^{4+}$$

which gives rise to longer straight chain polymers as the pH is increased. The solid ferric oxide begins to precipitate around pH 3. In the time frame of the experiments reported here, the hydrous ferric oxide reaches what appear to be two equilibrium stages, one at about two hours and another at about 24 hours. The first corresponds to separation of the solid in its most hydrated state. The second occurs after the polymers have completed fast olation and oxolation processes. It is likely that a third stage follows in which there is very slow dehydration of the solid with increasing cross-

linking and crystallinity. Byrne and Kester (13) found evidence for increasing crystallinity after very long aging periods for amorphous ferric oxide.

The loose, highly hydrated structure of the ferric oxide used in this work readily accommodates foreign ions which become incorporated into the solid as they hydrolyze. A loss of H^+ accompanies the formation of -OH and -O- bridges. The observed effect of chloride is a consequence of the formation of complexes with the metal ions which are not incorporated into the solid. Rudnev et al. (41) found a similar effect of NH_3 on copper coprecipitation with ferric hydrous oxide.

In addition to accounting for the high capacity of the iron for metals, this image also provides an explanation for the similarity between isotherms obtained by precipitation of the iron in the presence and absence of Cu^{2+}. It is also consistent with what is known regarding the formation of metal ferrites (42). The amorphous complex oxides, such as those obtained in this work, are precursors of the crystalline ferrites. Adamovich et al. (43) examined the solid resulting from the coprecipitation of Fe and Cu by X-ray diffraction and thermogravimetry and found evidence for a single solid phase rather than a mixture of iron and copper oxides. Heating the solid produced a compound whose X-ray diffraction pattern was suggestive of copper ferrite. Gmelin (44) documents the preparation of copper ferrite by heating a coprecipitated iron and copper oxides. When the oxides are precipitated separately, mixed, and heated only CuO and Fe_2O_3 are formed.

The results of this study show that despite its complexity, the amorphous iron oxide in seawater system behaves rather simply. The removal of metal can be approximately predicted under all concentration and electrolyte conditions by a constant which is only a function of pH. This pH dependence can presumably be accounted for in a numerical model by adjusting the acid-base chemistry of the solid which is difficult to quantitate experimentally. Although the mathematics appears to be similar to the surface complexation model for adsorption on crystalline metal oxides, the reaction between amorphous iron oxide and metals should not be viewed as a macroscopic surface phenomenon. In many ways, amphorous ferric oxide can be viewed as more closely analogous to polyelectrolytes than to crystalline solids such as quartz.

REFERENCES

1. Krauskopf, Konrad B. Geochim. et Cosmochim. Acta, 9:1, 1956.

2. Goldberg, E.D. J. Geology, 62:249, 1954.

3. Goldschmidt, V.M. J. Chem. Soc., 1937:655, 1937.

4. Forbes, E.A., A. Posner, and J.P. Quirk. J. Colloid Interface Sci., 49(3), 1974.

5. Yates, D.E., and T.W. Healy. J. Colloid Interface Sci., 52(2):222, 1975.

6. Dousma, J., and P.L. deBruyn. J. Colloid Interface Sci., 56(3):527, 1976.

7. Kolthoff, I.M., and B. Moskovitz. J. Phys. Chem., 41:629, 1937.

8. Parks, G.A., and P.L. deBruyn. J. Phys. Chem., 66:967, 1962.

9. Atkinson, R.J., Posner, A.M., and J.P. Quirk. J. Phys. Chem., 71(3), 1967.

10. Gadde, R.R., and H.A. Laitinen. Environ. Lett., 5(4):223, 1973.

11. Ellis, J., R. Giovanoli, and W. Stumm. Chimia, 30:194, 1976.

12. Murphy, P.J., A.M. Posner, and J.P. Quirk. J. Colloid Interface Sci., 56(2):270, 1976.

13. Byrne, R.H., and D.R. Kester. Marine Chem., 4:255, 1976.

14. Stumm, W. Personal communication.

15. Kurbatov, J.D., J.L. Kulp, and E. Mack, Jr. J. Am. Chem. Soc., 67:1923, 1945.

16. Gadde, R.R., and H.A. Laitinen. Anal. Chem., 46(13):2022, 1974.

17. McNaughton, M.G., and R.O. James. J. Colloid Interface Sci., 47(2):431, 1974.

18. O'Connor, T.P., and D.R. Kester. Geochim. et Cosmochim Acta, 39:1531, 1975.

19. Forbes, E.A., A. Posner, and J.P. Quirk. J. Colloid Interface Sci.,

49(3), 1974.

20. Matijevic, E. In: Principles and Applications of Water Chemistry, Faust and Hunter.

21. James, R.O., and T.W. Healy. J. Colloid Interface Sci., 40(1):42, 1972.

22. Stanton, D.A., and R. duT. Burger. Geoderma, 1(1):13, 1967.

23. Vuceta, J. Ph.D Thesis, California Institute of Technology, 1976.

24. Brunauer, S., P.H. Emmett, and E. Teller. J. Am. Chem. Soc., 60:309, 1938.

25. James, R.O., P.J. Stiglich, and T.W. Healy. Faraday Disc. Chem. Soc., 59:142, 1976.

26. Kurbatov, J.D. J. Phys. Chem., 36:1241, 1932.

27. Breeuwsma, A., and J. Lyklema. J. Colloid Interface Sci., 43(2), 1973.

28. Kurbatov, J.D., J.L. Kulp, and E. Mack, Jr. J. Am. Chem. Soc., 67:1923, 1945.

29. Lyklema, J. Croatica Chem. Acta, 43:249, 1971.

30. Berube, Y.G., and P.L. deBruyn. J. Colloid Interface Sci., 27(2):305, 1968.

31. Breeuwsma, A., and J. Lyklema. Disc. of Faraday Soc., 52:324, 1971.

32. Yates, D.E., S. Levine, and T.W. Healy. J. Chem. Soc., 70:1807, 1974.

33. Stumm, W., H. Holh, and F. Dalang. Croatica Chem. Acta, 1976.

34. FWPCA Methods for Chemical Analysis of Water and Wastes, U.S. Dept. of Interior, 1969. p. 240.

35. Morel, F.M.M., J.C. Westall, J.G. Rueter, and J.P. Chaplick. Technical Note #16, Ralph M. Parsons Laboratory, M.I.T., Cambridge, Massachusetts, 1975.

36. Davis, J.A. Ph.D Thesis, Stanford University, 1977.

37. Britton, H.T.S. Hydrogen Ions, Vol. II. D. Van Nostrand and Co., Inc., Princeton, New Jersey, 1956.

38. Yates, D.E. Ph.D Thesis, University of Melbourne, 1975.

39. Parks, G.A. Adsorption in the Marine Environment. In: Chemical Oceanography, J.P. Riley and G. Skirrow, eds. Academic Press, London, 1975.

40. Walton, H.F. Principles and Methods of Chemical Analysis. Prentice-Hall, Inc., Englewood Cliffs, New Jersey, 1964.

41. Rudnev, N.A., G.I. Malofeeva, N.P. Andreeva, and T.V. Tikhonova. Zhurnal Anal. Khimmii, 26(4):697, 1971.

42. Hilpert, S., and A. Wille. Z. Physik. Chem., B-18:291, 1932.

43. Adamovich, T.P., V.V. Sviridov, and A.D. Lobanok. Dokl. Akad. Nauk. Belorussk. SSR, 8(5):312, 1964.

44. Gmelin's Handbuch der Anorganischen Chemie. Kupfer Teil B., Lief. 3, System Num. 60:1276, Verlag Chem., 1965.

TECHNICAL REPORT DATA
(Please read Instructions on the reverse before completing)

1. REPORT NO.	2.	3. RECIPIENT'S ACCESSION NO.
EPA-600/3-80-011		

4. TITLE AND SUBTITLE	5. REPORT DATE
ADSORPTION OF TRACE METALS BY HYDROUS FERRIC OXIDE IN SEAWATER	January 1980 issuing date
	6. PERFORMING ORGANIZATION CODE

7. AUTHOR(S)	8. PERFORMING ORGANIZATION REPORT NO.
Francois Morel and K. C. Swallow	

9. PERFORMING ORGANIZATION NAME AND ADDRESS	10. PROGRAM ELEMENT NO.
Ralph M. Parsons Laboratory for Water Resources and Hydrodynamics, Department of Civil Engineering Massachusetts Institute of Technology Cambridge, Massachusetts 02139	1BA819
	11. CONTRACT/GRANT NO. R803738

12. SPONSORING AGENCY NAME AND ADDRESS	13. TYPE OF REPORT AND PERIOD COVERED
Environmental Research Laboratory - Narragansett, R.I. Office of Research and Development U.S. Environmental Protection Agency Narragansett, Rhode Island 02882	Final
	14. SPONSORING AGENCY CODE EPA/600/05

15. SUPPLEMENTARY NOTES
---

16. ABSTRACT

The adsorption of trace metals by amorphous hydrous ferric oxide in seawater is studied with reference to simple model systems designed to isolate the factors which may have an effect on the isotherms. Results show that the complex system behaves in a remarkably simple way and that the data obtained under various conditions of total metal concentration and total oxide concentration can be reduced to an apparent reaction constant, K, which is a function of pH only. The high capacity of the oxide for trace metals renders the concept of a surface reaction useless to explain the uptake of metals. A physical picture of the oxide as a swollen hydrous gel permeable to hydrated ions is presented.

17. KEY WORDS AND DOCUMENT ANALYSIS

a. DESCRIPTORS	b. IDENTIFIERS/OPEN ENDED TERMS	c. COSATI Field/Group
Trace elements	Modelling Metalic Wastes	06/F

18. DISTRIBUTION STATEMENT	19. SECURITY CLASS *(This Report)*	21. NO. OF PAGES
RELEASE TO PUBLIC	UNCLASSIFIED	63
	20. SECURITY CLASS *(This page)*	22. PRICE
	UNCLASSIFIED	

EPA Form 2220-1 (9-73)

☆ U.S. GOVERNMENT PRINTING OFFICE 1980 -657-146/5546

United States
Environmental Protection
Agency

Environmental Research Information
Center
Cincinnati OH 45268

Postage and
Fees Paid
Environmental
Protection
Agency
EPA-335

Official Business
Penalty for Private Use, $300

Special Fourth-Class Rate
Book

Please make all necessary changes on the above label, detach or copy, and return to the address in the upper left-hand corner.

If you do not wish to receive these reports CHECK HERE ☐, detach, or copy this cover, and return to the address in the upper left-hand corner.

EPA-600/3-80-011